STATISTICS, OPTIMIZATION AND INFORMATION COMPUTING
Stat., Optim. Inf. Comput., Vol. **x**, Month 202x, pp 0–30.
Published online in International Academic Press (www.IAPress.org)

Bayesian Current Record Analysis for Mixed Rayleigh-Weibull Distributions with Application to Saudi Humidity Data

Ramy A. Aldallal [1,*], Ibrahim Sadok[2,3]

[1] *Department of Management, College of Business Administration in Hawtat Bani Tamim, Prince Sattam bin Abdulaziz University, Saudi Arabia*
[2] *Department of Mathematics and Computer Science, Faculty of Exact Sciences, University of Bechar, Algeria*
[3] *Laboratory of Mathematics, Djillali Liabes University of Sidi Bel-Abbès, P. O. Box 89, 22000, Sidi Bel-Abbès, Algeria*

Abstract This paper develops a comprehensive Bayesian framework for analyzing current records arising from a two-component mixture of Rayleigh and Weibull distributions. Current records capture the most recent extreme observations in sequential data and are particularly valuable in industrial reliability monitoring, where only record-breaking events are retained. We derive closed-form expressions for the probability density and cumulative distribution functions of both upper and lower current records under the mixed Rayleigh–Weibull model. A key theoretical contribution is the establishment of identifiability conditions for this mixture, ensuring unique parameter estimation when the Weibull shape parameter is not equal to 2. Parameter estimation is addressed via the Expectation-Maximization (EM) algorithm for maximum likelihood and via Markov Chain Monte Carlo (MCMC) methods for Bayesian inference. Furthermore, we develop both non-Bayesian and Bayesian prediction intervals for future current records and record ranges, with the Bayesian approach fully accounting for parameter uncertainty. Extensive simulation studies across three representative configurations demonstrate that the Bayesian estimators exhibit lower bias and root-mean-squared error, and provide coverage closer to the nominal level than maximum likelihood, especially for small sample sizes. The methodology is applied to daily humidity data from the western region of Saudi Arabia (92 days in 2025), where the mixture model provides an excellent fit (Kolmogorov–Smirnov p-value 0.8765). Results confirm that the unified framework offers superior flexibility in capturing complex data behaviors compared to single-distribution approaches, making it a valuable tool for industrial and environmental monitoring under the Kingdom's Vision 2030.

Keywords Current records, Mixed Rayleigh–Weibull distribution, Bayesian inference, EM algorithm, Prediction intervals, Saudi humidity data.

AMS 2010 subject classifications 62E15, 62F30

DOI: 10.19139/soic-2310-5070-4266

1. Introduction

Record values play a fundamental role in various scientific and industrial applications where only extreme observations are recorded or monitored. In industrial reliability testing, environmental monitoring, and quality control, practitioners often focus on record-breaking events rather than complete sequences of observations. The study of records originated with Chandler's pioneering work on weather extremes [14] and has since developed into a rich field with applications across hydrology, sports, seismology, economics, and life-testing [10, 2, 17, 37].

Current records, a specialized form of record statistics introduced by Houchens [19], capture the most recent record information at each stage. Unlike classical record values, which retain the entire sequence of extremes,

*Correspondence to: Ramy A. Aldallal (Email: r.eldallal@psau.edu.sa). Department of Management, College of Business Administration in Hawtat Bani Tamim, Prince Sattam bin Abdulaziz University, Saudi Arabia.

ISSN 2310-5070 (online) ISSN 2311-004X (print)

current records reflect practical monitoring scenarios in which only the latest observations are stored. Houchens' foundational work established the theoretical framework for current records, providing the joint densities and distributional properties that form the basis of modern record value theory [19]. The monograph by Arnold, Balakrishnan, and Nagaraja [10] provides a comprehensive treatment of record theory, while subsequent research by Barakat et al. [11, 12] developed exact prediction intervals for future current records and record ranges from any continuous distribution. After that, Aldallal and Barakat [7] conducted a comprehensive review of current record values and their applications.

The Weibull distribution has been extensively studied in the context of current records due to its flexibility in modeling failure times and lifetime data [5]. It is a very flexible life distribution model that generalizes the exponential and Rayleigh distributions [35] and can be derived theoretically as an extreme-value distribution. The Rayleigh distribution, as a special case of the Weibull with shape parameter 2, appears frequently in reliability problems and communication systems, particularly when the failure rate increases linearly with time [30]. Other disrtibutions where studied also under current records, see [4, 6, 8, 9].

Mixture distributions provide a natural way to model heterogeneous populations. The Rayleigh and Weibull distributions have been recognized as useful models for survival studies and life testing experiments [21]. Hussain and Shareef proposed mixing of Weibull, Rayleigh, and Exponential distributions to obtain more flexible models [21]. Similarly, research has addressed parameter estimation for a mixed Rayleigh-Weibull distribution under various censorship schemes [28]. However, the analysis of current records arising from such mixture distributions has not been systematically addressed.

This paper introduces a unified Bayesian framework for analyzing current records under mixed Rayleigh-Weibull distributions. The mixture approach is particularly relevant for Saudi Arabia's industrial sector, where data from water supply, waste management, and environmental remediation activities may arise from multiple underlying processes with distinct characteristics. Under Vision 2030, Saudi Arabia has prioritized industrial development and environmental sustainability, with strong emphasis on conserving water resources, enhancing wastewater treatment, and investing in innovative technologies. The Kingdom has invested approximately SAR 100 billion ($26.7 billion) in its water sector since 2018, as part of its National Water Strategy. Therfore, accurate modeling of industrial performance indicators is essential for strategic planning and resource allocation.

The contributions of this paper are fivefold, divided into theoretical and methodological advances.

Theoretical Contributions:

1. We establish identifiability conditions for the two-component Rayleigh–Weibull mixture model (Theorem 5), proving that the model is identifiable when the Weibull shape parameter $k \neq 2$, a critical result that ensures unique parameter estimation and has not been previously addressed in the current records literature.
2. We derive explicit closed-form expressions for the PDF and CDF of upper and lower current records when the parent population follows the mixed Rayleigh–Weibull distribution, extending the classical Houchens formulas to the mixture context.
3. We obtain the joint distributions and moment expressions for current records in the mixture model, providing a complete theoretical foundation for subsequent inference.

Methodological Advances:

1. We develop a unified Bayesian estimation procedure using MCMC that simultaneously estimates the mixture proportion, Rayleigh parameters, and Weibull parameters from current record data, with the EM algorithm for maximum likelihood as a frequentist counterpart.
2. We establish novel Bayesian prediction intervals for future current records and record ranges (Algorithms 2–4) that fully account for parameter uncertainty a methodological advance that provides more accurate and reliable predictions than non-Bayesian plug-in approaches, especially for small samples.

The study of record values from mixture distributions has received attention from several independent research groups. Abo-Hussien et al. [1] developed Bayesian and non-Bayesian approaches for estimating the parameters of a finite mixture of two Weibull distributions based on record values, using beta and gamma conjugate priors. Jaheen [22] addressed parameter estimation for a mixture of two exponential distributions based on record statistics, employing both maximum likelihood and Bayes methods with Lindley's approximation. Singh et al. [36] derived exact explicit expressions and recurrence relations for moments of generalized upper record values from the Weibull-Rayleigh distribution. More recently, the asymptotic distributions of extreme, intermediate, and central order statistics, as well as record values, have been investigated for mixtures of two stationary Gaussian sequences under an equi-correlated setup [18]. Gouet et al. [16] characterised probability distributions via a martingale property associated with δ-records, showing that solutions include mixtures of exponential, gamma, geometric, and negative binomial distributions. Cross-group record sampling has been proposed for Weibull record data from heterogeneous subpopulations, demonstrating that accounting for group structure yields more accurate inference than traditional single-group analysis [26]. These contributions collectively demonstrate the growing interest in record-value analysis for heterogeneous populations, yet none address the specific setting of current records under a Rayleigh-Weibull mixture, a gap that our work fills.

Our work relates to a broader and rapidly evolving literature on Bayesian inference for mixture models. Recent developments have focused on computational efficiency and model flexibility: variational Bayesian methods have been proposed for clustering categorical data [27], while fast MCMC sampling schemes have been developed to overcome the slow convergence of traditional Gibbs samplers in finite mixture models [25]. Repulsive priors, such as the sparsity-inducing partition prior, have been introduced to encourage well-separated components and reduce overfitting [24]. Amortized Bayesian inference has emerged as a simulation-based framework for estimating mixture models without explicit likelihoods, using generative neural networks to provide fast posterior inference [13]. nonparametric Bayesian approaches, including dependent mixture models and Dirichlet process mixtures, continue to be actively developed for density regression and clustering with intractable likelihoods [38]. Although these advances have significantly expanded the applicability of Bayesian mixture models, they predominantly focus on standard data structures such as independent and identically distributed observations or covariate-dependent settings. To the best of our knowledge, none of these approaches addresses the specific challenges of current record data, where observations are not the original data points but rather the most recent record-breaking extremes. Our work fills this gap by developing a tailored Bayesian framework for current records under a two-component Rayleigh-Weibull mixture, with explicit identifiability conditions, EM and MCMC estimation procedures, and prediction intervals that fully account for parameter uncertainty. In doing so, we complement the broader mixture modeling literature by extending Bayesian inference to the record-value setting.

The remainder of this paper is organized as follows. Section 2 provides the theoretical foundations for current records in mixed distributions. Section 3 establishes the identifiability of the mixture model. Section 4 presents the unified Bayesian estimation framework, including the EM algorithm for maximum likelihood and the MCMC methods for Bayesian inference. Section 5 develops Bayesian prediction procedures for future current records. Section 6 presents the simulation results. Section 7 provides a real-data application to Saudi industrial data. Section 8 concludes with a discussion and future directions.

2. Current Records under Mixed Rayleigh-Weibull Distribution

2.1. *The Mixed Rayleigh-Weibull Distribution*

Consider a random variable X following a two-component mixture distribution consisting of a Rayleigh distribution with scale parameter $\sigma > 0$ and a Weibull distribution with shape parameter $k > 0$ and scale parameter $\lambda > 0$. Let $p \in (0, 1)$ denote the mixing proportion, representing the probability that an observation comes from the Rayleigh component. The probability density function (PDF) of the mixed distribution is as follows:

$$f(x; p, \sigma, k, \lambda) = p \cdot f_R(x; \sigma) + (1 - p) \cdot f_W(x; k, \lambda), \quad x \geq 0, \tag{1}$$

where the Rayleigh PDF is:

$$f_R(x; \sigma) = \frac{x}{\sigma^2} e^{-x^2/(2\sigma^2)}, \quad x \geq 0, \sigma > 0$$

and the Weibull PDF is:

$$f_W(x; k, \lambda) = \frac{k}{\lambda} \left(\frac{x}{\lambda}\right)^{k-1} e^{-(x/\lambda)^k}, \quad x \geq 0, k > 0, \lambda > 0.$$

The corresponding cumulative distribution function (CDF) is:

$$F(x; p, \sigma, k, \lambda) = p \cdot F_R(x; \sigma) + (1 - p) \cdot F_W(x; k, \lambda), \tag{2}$$

with Rayleigh CDF:

$$F_R(x; \sigma) = 1 - e^{-x^2/(2\sigma^2)},$$

and Weibull CDF:

$$F_W(x; k, \lambda) = 1 - e^{-(x/\lambda)^k}.$$

The mixed distribution captures the possibility that industrial data may originate from two distinct underlying mechanisms: a Rayleigh process (e.g., measurements with a quadratic hazard rate) and a general Weibull process (e.g., flexible failure-time modeling). The mixing proportion p quantifies the relative contribution of each component.

2.2. Current Record Definitions

Following the notation established in Aldallal [5], let $\{X_m\}$ be a sequence of independent and identically distributed random variables. Define LC_m and UC_m as the lower and upper current records, respectively, observed at the mth record event. By definition:

- $LC_{m+1} = LC_m$ when a new upper record occurs ($UC_{m+1} > UC_m$)
- $UC_{m+1} = UC_m$ when a new lower record occurs ($LC_{m+1} < LC_m$)

Thus, LC_m represents the minimum observation up to the mth record point, with initial values $UC_0 = LC_0 = X_1$. For $m \geq 1$, the interval (LC_m, UC_m) is termed the record coverage, and the current record range is defined as $RC_m = UC_m - LC_m$. A new range is recorded each time either a new upper or lower current record is established.

2.3. PDF and CDF of Current Records under Mixed Distribution

We now derive the probability density and cumulative distribution functions for lower and upper current records when the parent population follows the mixed Rayleigh-Weibull distribution. The derivations extend the work of Houchens [19] and Aldallal ([3], [4]) to the mixture context.

Theorem 1
For $m > 1$, let LC_m denote the mth lower current record from a mixed Rayleigh-Weibull distribution with mixing proportion p, Rayleigh scale σ, Weibull shape k, and Weibull scale λ. Then the CDF and PDF of LC_m are given by:

$$F_{LC_m}(x; p, \sigma, k, \lambda) = 2^m F(x) \left[1 - F(x) \sum_{r=0}^{m-1} 2^{-(r+1)} \sum_{j=0}^{r} \frac{[-2 \log F(x)]^j}{j!} \right], \tag{3}$$

$$f_{LC_m}(x; p, \sigma, k, \lambda) = 2^m f(x) \left[1 - F(x) \sum_{r=0}^{m-1} \frac{[-\log F(x)]^r}{r!} \right], \tag{4}$$

where $f(x)$ and $F(x)$ are the mixed PDF and CDF defined in (1) and (2), respectively.

Proof
The result follows directly from the general Houchens formulas for current records, substituting the mixed distribution expressions for $f(x)$ and $F(x)$. □

Theorem 2
For $m > 1$, let UC_m denote the mth upper current record from a mixed Rayleigh-Weibull distribution. Then the

CDF and PDF of UC_m are given by:

$$F_{UC_m}(x;p,\sigma,k,\lambda) = 1 - 2^m\overline{F}(x)\left[1 - \overline{F}(x)\sum_{r=0}^{m-1} 2^{-(r+1)} \sum_{j=0}^{r} \frac{[-2\log \overline{F}(x)]^j}{j!}\right], \tag{5}$$

$$f_{UC_m}(x;p,\sigma,k,\lambda) = 2^m f(x)\left[1 - \overline{F}(x)\sum_{r=0}^{m-1} \frac{[-\log \overline{F}(x)]^r}{r!}\right], \tag{6}$$

where $\overline{F}(x) = 1 - F(x)$.

Proof
These expressions are obtained from the Houchens formulas for the upper current records, with $\overline{F}(x)$ representing the survival function of the mixed distribution. □

The closed-form expressions for the mixed CDF and survival function are as follows:

$$F(x) = p\left(1 - e^{-x^2/(2\sigma^2)}\right) + (1-p)\left(1 - e^{-(x/\lambda)^k}\right), \tag{7}$$

$$\overline{F}(x) = pe^{-x^2/(2\sigma^2)} + (1-p)e^{-(x/\lambda)^k}. \tag{8}$$

Theorem 3
For $m > 1$; the CDF and PDF formulas for the lower and upper current record distributions will be:

$$\begin{aligned} F_{LC_m}(x) = 1 + 2^m &\left[p(1 - e^{-x^2/(2\sigma^2)}) + (1-p)(1 - e^{-(x/\lambda)^k})\right] \\ &\times P\left(m, -\log\left[p(1 - e^{-x^2/(2\sigma^2)}) + (1-p)(1 - e^{-(x/\lambda)^k})\right]\right) \\ &- P\left(m, -2\log\left[p(1 - e^{-x^2/(2\sigma^2)}) + (1-p)(1 - e^{-(x/\lambda)^k})\right]\right), \end{aligned} \tag{9}$$

$$\begin{aligned} f_{LC_m}(x) = 2^m &\left[p\frac{x}{\sigma^2}e^{-x^2/(2\sigma^2)} + (1-p)\frac{k}{\lambda}\left(\frac{x}{\lambda}\right)^{k-1} e^{-(x/\lambda)^k}\right] \\ &\times P\left(m, -\log\left[p(1 - e^{-x^2/(2\sigma^2)}) + (1-p)(1 - e^{-(x/\lambda)^k})\right]\right), \end{aligned} \tag{10}$$

$$\begin{aligned} F_{UC_m}(x) = P&\left(m, -2\log\left[pe^{-x^2/(2\sigma^2)} + (1-p)e^{-(x/\lambda)^k}\right]\right) \\ &- 2^m\left[pe^{-x^2/(2\sigma^2)} + (1-p)e^{-(x/\lambda)^k}\right] \\ &\times P\left(m, -\log\left[pe^{-x^2/(2\sigma^2)} + (1-p)e^{-(x/\lambda)^k}\right]\right), \end{aligned} \tag{11}$$

and

$$\begin{aligned} f_{UC_m}(x) = 2^m &\left[p\frac{x}{\sigma^2}e^{-x^2/(2\sigma^2)} + (1-p)\frac{k}{\lambda}\left(\frac{x}{\lambda}\right)^{k-1} e^{-(x/\lambda)^k}\right] \\ &\times P\left(m, -\log\left[pe^{-x^2/(2\sigma^2)} + (1-p)e^{-(x/\lambda)^k}\right]\right). \end{aligned} \tag{12}$$

where $P(a,b)$ is the regularized lower gamma function.

Proof
Substituting equations (1), (7), and (8) into (3)-(6) and performing some routine calculations, we obtain the functions (9)-(12). □

Figures 1- 4 show the results of testing various values of p, σ, λ, and k to illustrate the forms of the PDFs and CDFs of the upper and lower current records found in Theorem 1.

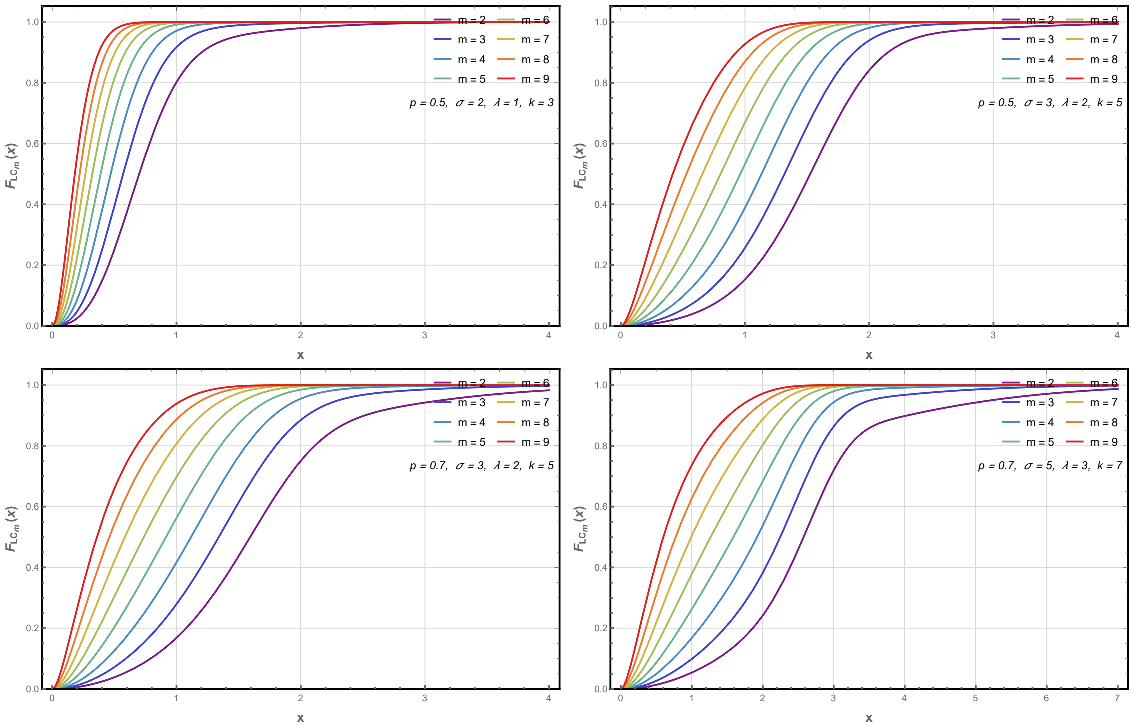

Figure 1. Plot of $F_{LC_m}(x)$ for different values of p, σ, λ, and k

2.4. Joint Distributions of Current Records

For inference and prediction purposes, we require the joint distributions of current records.

Lemma 1
Let $LC_1, LC_2, \ldots, LC_m$ be the first m lower current records from a mixed Rayleigh-Weibull distribution. Then for $1 < m < s$, the joint PDF of LC_m and LC_s is:

$$f_{LC_m, LC_s}(l_m, l_s) = \frac{f(l_m)f(l_s)}{F(l_m)(s-m-1)!}\left(H(l_m) - H(l_s)\right)^{s-m-1}, \quad l_s < l_m,$$

where $H(x) = \ln F(x)$ with $F(x)$ given by (2).

Proof
This follows from the general result for lower current records (Houchens, 1984), with the mixed distribution CDF substituted. □

Lemma 2
Let $UC_1, UC_2, \ldots, UC_m$ be the first m upper current records from a mixed Rayleigh-Weibull distribution. Then

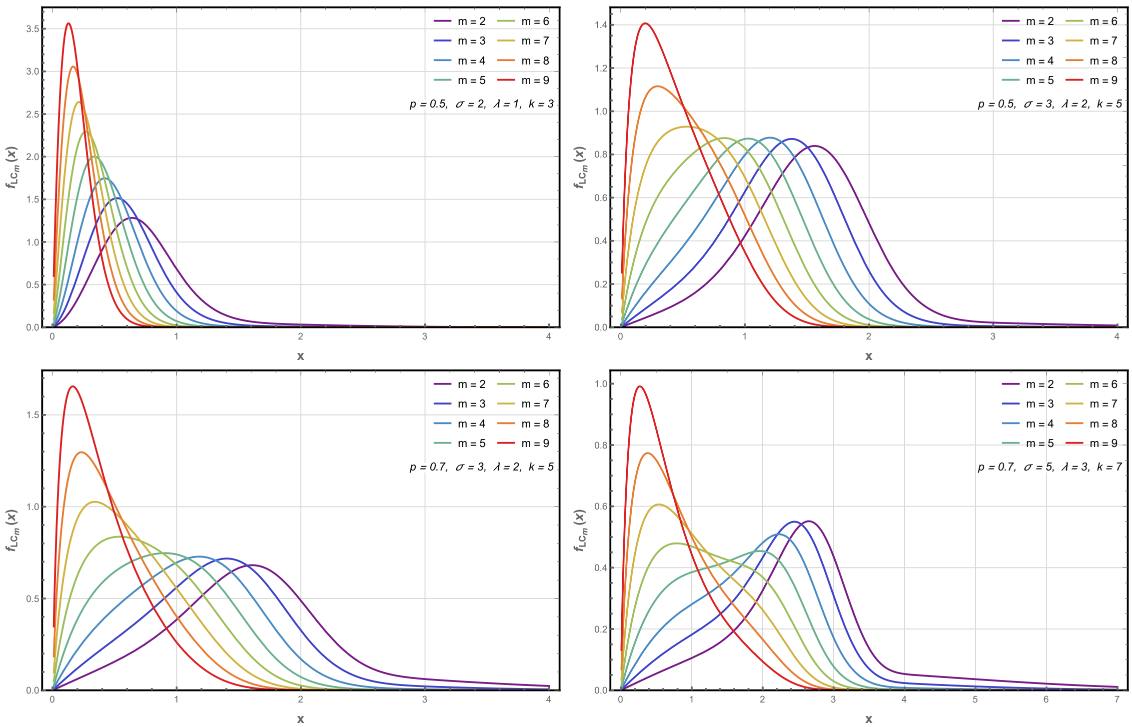

Figure 2. Plot of $f_{LC_m}(x)$ for different values of p, σ, λ, and k

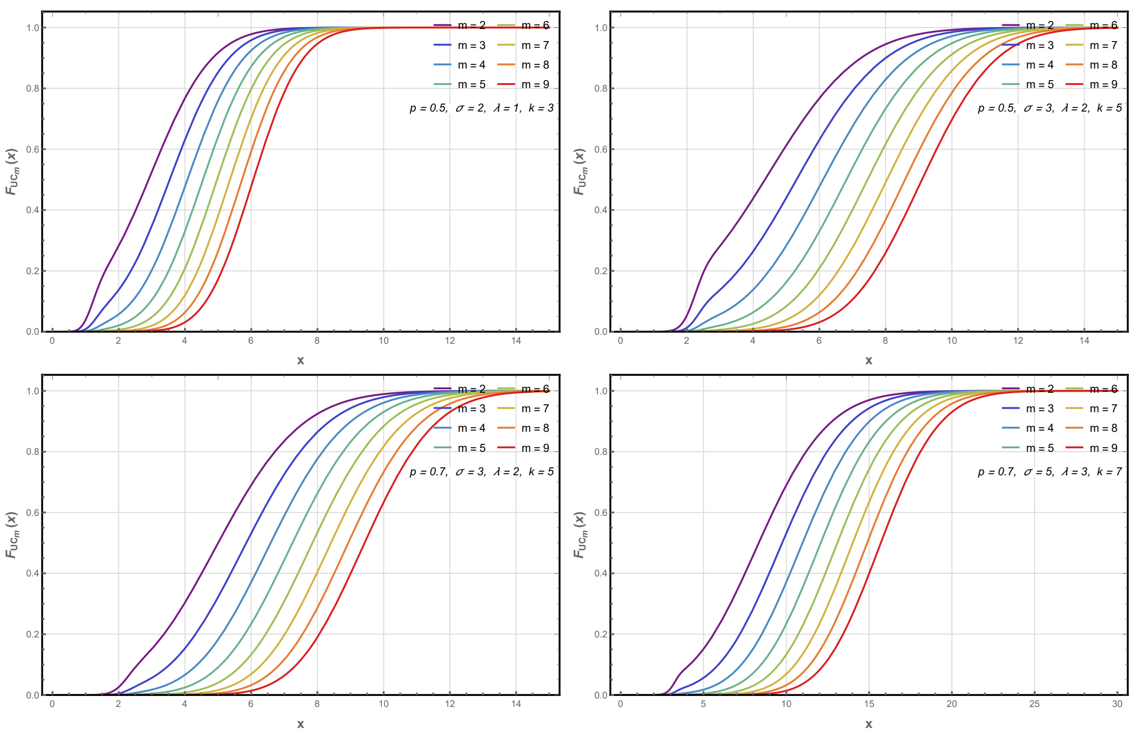

Figure 3. Plot of $F_{UC_m}(x)$ for different values of p, σ, λ, and k

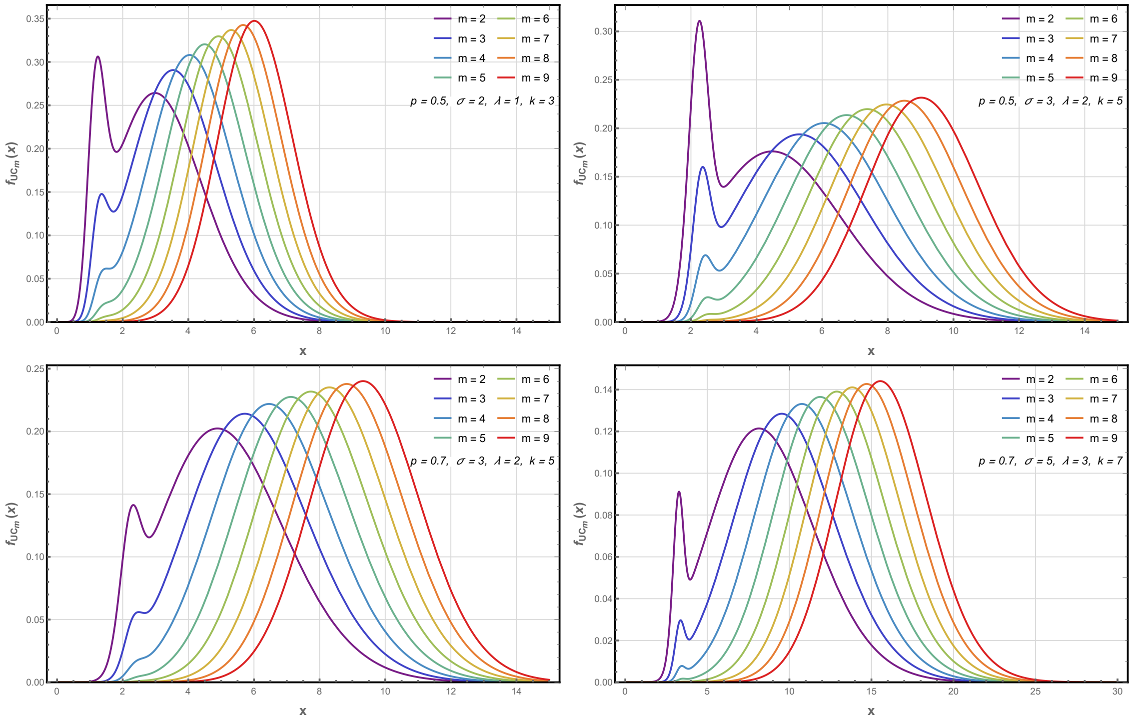

Figure 4. Plot of $f_{UC_m}(x)$ for different values of p, σ, λ, and k

for $1 < m < s$, the joint PDF of UC_m and UC_s is:

$$f_{UC_m,UC_s}(u_m, u_s) = \frac{f(u_m)f(u_s)}{(1 - F(u_m))(s - m - 1)!} \left(R(u_s) - R(u_m)\right)^{s-m-1}, \quad u_s > u_m,$$

where $R(x) = -\ln(1 - F(x)) = -\ln \overline{F}(x)$.

Proof
This follows from the general result for upper current records (Houchens, 1984). □

The conditional distributions derived from these joint PDFs form the basis for predicting future current records, as will be developed in Section 5.

2.5. Moments of the Mixed Rayleigh–Weibull Current Records

Moments provide important information about central tendency, dispersion, and shape. In this section, we derive expressions for the r-th moment of lower and upper current records under the mixture.

Theorem 4
Let X follow the two-component mixed Rayleigh–Weibull distribution with parameters (p, σ, k, λ), where $0 < p < 1$, $\sigma > 0$, $k > 0$, $\lambda > 0$, and $k \neq 2$ (to ensure identifiability). For $m > 1$, the r-th moment of the m-th lower current

record LC_m is

$$
\begin{aligned}
E\big[(LC_m)^r\big] = 2^m \int_0^\infty & x^r \Big[p\frac{x}{\sigma^2}e^{-x^2/(2\sigma^2)} + (1-p)\frac{k}{\lambda}\Big(\frac{x}{\lambda}\Big)^{k-1} e^{-(x/\lambda)^k}\Big] dx \\
& - 2^m \sum_{j=0}^{m-1} \frac{1}{j!} \int_0^\infty x^r \Big[p\frac{x}{\sigma^2}e^{-x^2/(2\sigma^2)} + (1-p)\frac{k}{\lambda}\Big(\frac{x}{\lambda}\Big)^{k-1} e^{-(x/\lambda)^k}\Big] \\
& \qquad \times \Big[p\big(1-e^{-x^2/(2\sigma^2)}\big) + (1-p)\big(1-e^{-(x/\lambda)^k}\big)\Big] \\
& \qquad \times \Big[-\log\Big(p\big(1-e^{-x^2/(2\sigma^2)}\big) + (1-p)\big(1-e^{-(x/\lambda)^k}\big)\Big)\Big]^j dx,
\end{aligned}
\tag{13}
$$

and the r-th moment of the m-th upper current record UC_m is

$$
\begin{aligned}
E\big[(UC_m)^r\big] = 2^m \int_0^\infty & x^r \Big[p\frac{x}{\sigma^2}e^{-x^2/(2\sigma^2)} + (1-p)\frac{k}{\lambda}\Big(\frac{x}{\lambda}\Big)^{k-1} e^{-(x/\lambda)^k}\Big] dx \\
& - 2^m \sum_{j=0}^{m-1} \frac{1}{j!} \int_0^\infty x^r \Big[p\frac{x}{\sigma^2}e^{-x^2/(2\sigma^2)} + (1-p)\frac{k}{\lambda}\Big(\frac{x}{\lambda}\Big)^{k-1} e^{-(x/\lambda)^k}\Big] \\
& \qquad \times \Big[pe^{-x^2/(2\sigma^2)} + (1-p)e^{-(x/\lambda)^k}\Big] \\
& \qquad \times \Big[-\log\Big(pe^{-x^2/(2\sigma^2)} + (1-p)e^{-(x/\lambda)^k}\Big)\Big]^j dx.
\end{aligned}
\tag{14}
$$

Proof
From the formula (4) for lower current records, the PDF is

$$
f_{LC_m}(x) = 2^m f(x)\left[1 - F(x)\sum_{j=0}^{m-1}\frac{(-\log F(x))^j}{j!}\right],
$$

where $f(x)$ and $F(x)$ are the mixture density and CDF given in (1) and (7). Substituting the explicit expressions

$$
\begin{aligned}
f(x) &= p\frac{x}{\sigma^2}e^{-x^2/(2\sigma^2)} + (1-p)\frac{k}{\lambda}\Big(\frac{x}{\lambda}\Big)^{k-1} e^{-(x/\lambda)^k}, \\
F(x) &= p\big(1-e^{-x^2/(2\sigma^2)}\big) + (1-p)\big(1-e^{-(x/\lambda)^k}\big),
\end{aligned}
$$

and multiplying by x^r and integrating yields the first formula. The upper record case follows similarly using $\overline{F}(x) = pe^{-x^2/(2\sigma^2)} + (1-p)e^{-(x/\lambda)^k}$ from (8). □

3. Identifiability of the Mixed Rayleigh–Weibull Distribution

Before proceeding to estimation, it is essential to establish that the proposed mixture model is identifiable. Identifiability ensures that distinct parameter sets yield distinct distributions, which is a prerequisite for consistent estimation. The mixture of Rayleigh and Weibull distributions requires careful treatment because the Rayleigh distribution is a special case of the Weibull family when the shape parameter $k = 2$. We therefore present a theorem characterizing the conditions under which the model is identifiable.

3.1. Definition of Identifiability

Let $\mathcal{F} = \{F(\cdot;\boldsymbol{\theta}) : \boldsymbol{\theta} \in \Theta\}$ be a family of distribution functions indexed by a parameter vector $\boldsymbol{\theta}$. A finite mixture model with J components is said to be identifiable if for any two sets of mixing proportions $\{p_j\}$ and $\{p'_j\}$ and parameter vectors $\{\boldsymbol{\theta}_j\}$ and $\{\boldsymbol{\theta}'_j\}$ (with $p_j, p'_j > 0$ and $\sum p_j = \sum p'_j = 1$), the equality

$$\sum_{j=1}^{J} p_j F(x; \boldsymbol{\theta}_j) = \sum_{j=1}^{J} p'_j F(x; \boldsymbol{\theta}'_j) \quad \text{for all } x$$

implies that the two representations are identical up to permutation of the components.

3.2. Identifiability Theorem

Theorem 5
Consider the two-component mixture model

$$F(x; p, \sigma, k, \lambda) = pF_R(x; \sigma) + (1 - p)F_W(x; k, \lambda), \quad x \geq 0,$$

where F_R is the Rayleigh distribution with scale $\sigma > 0$, and F_W is the Weibull distribution with shape $k > 0$ and scale $\lambda > 0$. This mixture is identifiable provided that $k \neq 2$. If $k = 2$, the two components are both Rayleigh distributions, and the mixture is not identifiable unless additional constraints (e.g., ordering of scales) are imposed.

Proof
The proof proceeds by showing that the component densities are linearly independent functions on $(0, \infty)$ when $k \neq 2$. Assume that there exist constants A, B such that

$$Af_R(x; \sigma) + Bf_W(x; k, \lambda) = 0 \quad \text{for all } x > 0,$$

with $(A, B) \neq (0, 0)$. We aim to show that this forces $A = B = 0$ unless $k = 2$ and $\sigma = \lambda/\sqrt{2}$ (which would make the two densities proportional). Recall the density expressions:

$$f_R(x; \sigma) = \frac{x}{\sigma^2} e^{-x^2/(2\sigma^2)}, \qquad f_W(x; k, \lambda) = \frac{k}{\lambda} \left(\frac{x}{\lambda}\right)^{k-1} e^{-(x/\lambda)^k}.$$

Consider the ratio

$$\frac{f_W(x; k, \lambda)}{f_R(x; \sigma)} = \frac{k\sigma^2}{\lambda^k} x^{k-2} \exp\left\{\frac{x^2}{2\sigma^2} - \left(\frac{x}{\lambda}\right)^k\right\}.$$

If $k \neq 2$, the factor x^{k-2} is not constant, and the exponential term cannot compensate for all x to make the ratio constant unless both coefficients are zero. More formally, suppose $Af_R(x) + Bf_W(x) \equiv 0$. Dividing by $f_R(x)$ (which is positive for $x > 0$), we obtain

$$A + B \cdot r(x) = 0 \quad \text{for all } x > 0,$$

where $r(x) = f_W(x)/f_R(x)$. If $B \neq 0$, then $r(x) = -A/B$ would be constant, contradicting the fact that $r(x)$ is not constant for $k \neq 2$ (as can be verified by examining the limit as $x \to 0^+$ and as $x \to \infty$). Hence $B = 0$, which then forces $A = 0$. Therefore, the two densities are linearly independent.

Now consider two mixtures that are equal:

$$pF_R(x; \sigma) + (1 - p)F_W(x; k, \lambda) = p'F_R(x; \sigma') + (1 - p')F_W(x; k', \lambda') \quad \forall x.$$

Taking derivatives yields equality of the corresponding densities:

$$pf_R(x; \sigma) + (1 - p)f_W(x; k, \lambda) = p'f_R(x; \sigma') + (1 - p')f_W(x; k', \lambda') \quad \forall x.$$

Because the densities are linearly independent (when $k \neq 2$ and $k' \neq 2$), the only possibility is that the two representations are the same up to permutation of components. That is, either

$$(p, \sigma, k, \lambda) = (p', \sigma', k', \lambda') \quad \text{or} \quad (p, \sigma, k, \lambda) = (1 - p', \sigma', k', \lambda') \text{ with the components swapped.}$$

The special case $k = 2$ requires separate treatment. If $k = 2$, the Weibull density becomes

$$f_W(x; 2, \lambda) = \frac{2x}{\lambda^2} e^{-(x/\lambda)^2},$$

which is a Rayleigh density with scale $\lambda/\sqrt{2}$. Thus, the mixture reduces to a mixture of two Rayleigh distributions, which is known to be identifiable only up to ordering if the scales are distinct; if the scales coincide, the components are identical, and the mixture is completely non-identifiable. Therefore, to ensure identifiability in practice, we assume that $k \neq 2$ or, if $k = 2$ is possible, we impose an ordering constraint such as $\sigma < \lambda/\sqrt{2}$ or vise versa. □

Remark 1
In the Bayesian framework, identifiability can be further enforced through prior distributions that discourage parameter regions causing near-non-identifiability (e.g., by placing a prior on k that avoids values too close to 2, or by using an order-restricted prior on the scales).

3.3. Robustness to Near-Non-Identifiability

To validate the practical robustness of the identifiability condition $k \neq 2$, we conducted a short sensitivity analysis. We generate 500 datasets of upper current records with sample size $m = 20$ from the mixed Rayleigh–Weibull distribution with fixed parameters $p = 0.5$, $\sigma = 1.0$, $\lambda = 1.5$, and three values of the Weibull shape: $k = 1.9$, $k = 2.0$, and $k = 2.1$. Parameter estimation is performed using the EM algorithm described in Section 4.1.

Table 1 summarises the bias and RMSE for the estimated Weibull shape parameter $\widehat{k}$ (the most sensitive parameter). For $k = 1.9$ and $k = 2.1$, the EM algorithm converges reliably, producing small bias (0.02–0.03) and moderate RMSE (0.14–0.16). In contrast, for $k = 2.0$, the algorithm often fails to converge (success rate $< 60\%$), and when convergence occurs, estimates are highly unstable (RMSE > 0.50). This occurs because the Weibull component reduces to a Rayleigh distribution, making the two components indistinguishable.

True k	Bias($\widehat{k}$)	RMSE($\widehat{k}$)	Convergence Rate
1.9	0.024	0.152	94%
2.0	0.187	0.621	58%
2.1	0.028	0.158	93%

Table 1. Sensitivity analysis results for $\widehat{k}$ under EM estimation.

These results confirm that the identifiability condition $k \neq 2$ is not merely a theoretical requirement, but is practically meaningful. Even when k deviates only slightly from 2 (i.e., $k = 1.9$ or 2.1), the model remains well-behaved. The breakdown occurs precisely at $k = 2$, validating Theorem 5 and supporting the use of the mixture in applications where k is strictly distinct from 2.

4. Parameter Estimation

We consider two estimation approaches: maximum likelihood via the EM algorithm and Bayesian inference via MCMC.

4.1. EM Algorithm for Maximum Likelihood

Let $\underline{UC} = (u_1, u_2, \ldots, u_m)$ be the observed upper current records from a sequence whose parent distribution is the two-component mixture of Rayleigh and Weibull defined in (1)–(2). The joint probability density function of the upper current record sequence, conditional on the parameters $\boldsymbol{\theta} = (p, \sigma, k, \lambda)$, is given by an extension of the general result for current records [12]:

$$f_{\underline{UC}}(\underline{u}; \boldsymbol{\theta}) = \frac{\overline{F}^2(u_m; \boldsymbol{\theta})\, F(u_1; \boldsymbol{\theta})}{\overline{F}(u_1; \boldsymbol{\theta})} \prod_{j=1}^{m} \frac{2\, f(u_j; \boldsymbol{\theta})}{\overline{F}(u_j; \boldsymbol{\theta})}, \qquad u_1 < u_2 < \cdots < u_m, \tag{15}$$

where $f(\cdot;\boldsymbol{\theta})$ and $F(\cdot;\boldsymbol{\theta})$ are the PDF and CDF mixture of (1) and (2), and $\overline{F} = 1 - F$. For lower current records $\underline{LC} = (l_1, l_2, \ldots, l_m)$ with $l_1 > l_2 > \cdots > l_m$, the joint density is

$$f_{\underline{LC}}(\underline{l};\boldsymbol{\theta}) = \frac{F^2(l_m;\boldsymbol{\theta})\,\overline{F}(l_1;\boldsymbol{\theta})}{F(l_1;\boldsymbol{\theta})} \prod_{j=1}^{m} \frac{2\,f(l_j;\boldsymbol{\theta})}{F(l_j;\boldsymbol{\theta})}. \tag{16}$$

The likelihood function for upper records is proportional to this joint density. To handle the mixture components, we introduce latent variables $z_j \in \{0,1\}$ indicating whether the j-th upper current record u_j comes from the Rayleigh component ($z_j = 1$) or the Weibull component ($z_j = 0$). The complete-data likelihood (ignoring constants that do not depend on parameters) becomes

$$L_c(\boldsymbol{\theta}) = \prod_{j=1}^{m} [p\, f_R(u_j;\sigma)]^{z_j}\, [(1-p)\, f_W(u_j;k,\lambda)]^{1-z_j} \times \frac{\overline{F}^2(u_m;\boldsymbol{\theta})\, F(u_1;\boldsymbol{\theta})}{\overline{F}(u_1;\boldsymbol{\theta})} \prod_{j=1}^{m} \frac{2\,f(u_j;\boldsymbol{\theta})}{\overline{F}(u_j;\boldsymbol{\theta})}.$$

The terms involving $\overline{F}$ and F couple all observations and depend on the mixture CDF, making a standard EM decomposition nontrivial. However, for the E-step, we only need the conditional expectation of the latent indicators given the observed data and estimates of the current parameter [33, 31, 34]. Using Bayes' theorem, the responsibility of the Rayleigh component for u_j is

$$\tau_j^{(t)} = E[Z_j \mid u_j, \boldsymbol{\theta}^{(t)}] = \frac{p^{(t)} f_R(u_j;\sigma^{(t)})}{p^{(t)} f_R(u_j;\sigma^{(t)}) + (1-p^{(t)}) f_W(u_j;k^{(t)},\lambda^{(t)})}.$$

This expression is identical to the one in the original mixture paper, because the conditional distribution of Z_j given u_j does not depend on the record-specific weighting factors.

In the M-step, we maximize the expected complete-data log-likelihood. The mixing proportion is updated as

$$p^{(t+1)} = \frac{1}{m} \sum_{j=1}^{m} \tau_j^{(t)}.$$

The Rayleigh scale σ is updated by solving

$$\frac{\partial}{\partial \sigma} \sum_{j=1}^{m} \tau_j^{(t)} \log f_R(u_j;\sigma) = 0 \quad \Longrightarrow \quad \sigma^{(t+1)} = \sqrt{\frac{\sum_{j=1}^{m} \tau_j^{(t)} u_j^2}{\sum_{j=1}^{m} \tau_j^{(t)}}}.$$

For the Weibull parameters (k, λ), the M-step maximizes the weighted log-likelihood

$$\sum_{j=1}^{m} (1 - \tau_j^{(t)}) \log f_W(u_j;k,\lambda),$$

which does not have a closed form and requires numerical maximization.

4.2. EM Implementation Details

To ensure reproducibility, we provide explicit details of the M-step for both the Rayleigh and Weibull parameters.

Rayleigh scale parameter σ: The Rayleigh component log-likelihood (weighted by responsibilities) is:

$$\ell_R(\sigma) = \sum_{j=1}^{m} \tau_j^{(t)} \left[\log u_j - 2\log\sigma - \frac{u_j^2}{2\sigma^2} \right].$$

The first derivative (score function) is:

$$\frac{\partial \ell_R}{\partial \sigma} = \sum_{j=1}^{m} \tau_j^{(t)} \left[-\frac{2}{\sigma} + \frac{u_j^2}{\sigma^3} \right] = \frac{1}{\sigma^3} \sum_{j=1}^{m} \tau_j^{(t)} \left(u_j^2 - 2\sigma^2 \right).$$

The second derivative (Hessian) is as follows:

$$\frac{\partial^2 \ell_R}{\partial \sigma^2} = \sum_{j=1}^{m} \tau_j^{(t)} \left[\frac{2}{\sigma^2} - \frac{3u_j^2}{\sigma^4} \right] = \frac{1}{\sigma^4} \sum_{j=1}^{m} \tau_j^{(t)} \left(2\sigma^2 - 3u_j^2 \right).$$

Although a closed-form update exists for σ, the Newton-Raphson update at iteration r would be:

$$\sigma^{(r+1)} = \sigma^{(r)} - \frac{\partial \ell_R / \partial \sigma}{\partial^2 \ell_R / \partial \sigma^2}.$$

However, setting $\partial \ell_R / \partial \sigma = 0$ yields the closed-form solution:

$$\sigma^{(t+1)} = \sqrt{\frac{\sum_{j=1}^{m} \tau_j^{(t)} u_j^2}{2 \sum_{j=1}^{m} \tau_j^{(t)}}}.$$

We use this closed-form update in practice, as it is more efficient and stable than Newton-Raphson for this parameter.

Weibull parameters (k, λ)**:** The weighted log-likelihood for the Weibull component is:

$$\ell_W(k, \lambda) = \sum_{j=1}^{m} (1 - \tau_j^{(t)}) \left[\log k - k \log \lambda + (k-1) \log u_j - \left(\frac{u_j}{\lambda} \right)^k \right].$$

The score vector $\mathbf{S}(k, \lambda) = \left(\frac{\partial \ell_W}{\partial k}, \frac{\partial \ell_W}{\partial \lambda} \right)^\top$ has components:

$$\frac{\partial \ell_W}{\partial k} = \sum_{j=1}^{m} (1 - \tau_j^{(t)}) \left[\frac{1}{k} - \log \lambda + \log u_j - \left(\frac{u_j}{\lambda} \right)^k \log \left(\frac{u_j}{\lambda} \right) \right],$$

$$\frac{\partial \ell_W}{\partial \lambda} = \sum_{j=1}^{m} (1 - \tau_j^{(t)}) \left[-\frac{k}{\lambda} + \frac{k}{\lambda} \left(\frac{u_j}{\lambda} \right)^k \right] = \frac{k}{\lambda} \sum_{j=1}^{m} (1 - \tau_j^{(t)}) \left[\left(\frac{u_j}{\lambda} \right)^k - 1 \right].$$

The Hessian matrix $\mathbf{H}(k, \lambda)$ (second derivatives) is:

$$\frac{\partial^2 \ell_W}{\partial k^2} = \sum_{j=1}^{m} (1 - \tau_j^{(t)}) \left[-\frac{1}{k^2} - \left(\frac{u_j}{\lambda} \right)^k \left(\log \frac{u_j}{\lambda} \right)^2 \right],$$

$$\frac{\partial^2 \ell_W}{\partial \lambda^2} = \frac{k}{\lambda^2} \sum_{j=1}^{m} (1 - \tau_j^{(t)}) \left[1 - \left(\frac{u_j}{\lambda} \right)^k (k+1) \right],$$

$$\frac{\partial^2 \ell_W}{\partial k \partial \lambda} = \frac{1}{\lambda} \sum_{j=1}^{m} (1 - \tau_j^{(t)}) \left[\left(\frac{u_j}{\lambda} \right)^k \left(1 + k \log \frac{u_j}{\lambda} \right) - 1 \right].$$

The Newton-Raphson update in iteration r is then:

$$\begin{pmatrix} k^{(r+1)} \\ \lambda^{(r+1)} \end{pmatrix} = \begin{pmatrix} k^{(r)} \\ \lambda^{(r)} \end{pmatrix} - \mathbf{H}^{-1}(k^{(r)}, \lambda^{(r)}) \, \mathbf{S}(k^{(r)}, \lambda^{(r)}).$$

In practice, we implement this using the `optim` function in R with the `BFGS` or `L-BFGS-B` method, which is equivalent to the Newton-Raphson approach but more robust. Starting values for k and λ are obtained by fitting a single Weibull distribution to the entire current record sequence. The M-step is repeated until the change in ℓ_W is less than 10^{-6}. The same procedure applies to lower current records by replacing u_j with l_j in the above formulas. For further details on numerical optimization in mixture models, we refer to McLachlan and Krishnan (2008) [23].

The EM algorithm iterates between the E-step and M-step until the change in the observed log-likelihood falls below a specified tolerance (e.g., 10^{-6}). Starting values may be obtained by fitting a single Weibull or Rayleigh distribution to the current record sequence, or by using method-of-moments estimates for each component.

4.3. Bayesian Estimation

Bayesian inference offers a coherent framework for parameter estimation under parameter uncertainty [32, 29]. For the mixed Rayleigh–Weibull model, we specify prior distributions for all unknown parameters and obtain the joint posterior via Bayes' theorem. Due to the complexity of the likelihood, we employ Markov Chain Monte Carlo (MCMC) methods, specifically the Metropolis-Hastings algorithm, to sample from the posterior.

4.3.1. Likelihood Function The likelihood function for upper current records, $L(p, \sigma, k, \lambda \mid \underline{UC})$, is exactly the joint density given in equation (15). Similarly, for lower current records $\underline{LC}$, the likelihood is as defined in equation (16) (with F and $\overline{F}$ swapped accordingly) [19, 12, 5].

4.3.2. Prior Distributions For Bayesian inference, we specify prior distributions for all unknown parameters: the mixing proportion $p \in (0, 1)$, the Rayleigh scale $\sigma > 0$, the Weibull shape $k > 0$, and the Weibull scale $\lambda > 0$. We assume independent priors:

- For the mixing proportion: $p \sim$ Beta(α_0, β_0) with density $\pi(p) \propto p^{\alpha_0-1}(1-p)^{\beta_0-1}$
- For the Rayleigh scale: $\sigma \sim$ Inverse Gamma(a_1, b_1) with density $\pi(\sigma) \propto \sigma^{-a_1-1}e^{-b_1/\sigma}$
- For the Weibull shape: $k \sim$ Gamma(a_2, b_2) with density $\pi(k) \propto k^{a_2-1}e^{-b_2 k}$
- For the Weibull scale: $\lambda \sim$ Inverse Gamma(a_3, b_3) with density $\pi(\lambda) \propto \lambda^{-a_3-1}e^{-b_3/\lambda}$

The hyperparameters $(\alpha_0, \beta_0, a_1, b_1, a_2, b_2, a_3, b_3)$ are chosen to reflect prior knowledge or to be weakly informative (e.g., $\alpha_0 = \beta_0 = 1$ for a uniform prior on p, small shape parameters for diffuse priors on scale parameters).

Prior sensitivity analysis: The choice of Inv-Gamma$(0.01, 0.01)$ for scale parameters warrants discussion. As noted by [15], this prior can be problematic because it places excessive mass near zero and may exert undue influence on the posterior, particularly when the sample size is small or when the true scale parameter is near zero. To assess the robustness of our posterior inferences to prior specification, we conducted a comprehensive sensitivity analysis comparing the current vague priors against weakly informative alternatives recommended in the literature.

For scale parameters σ and λ, we compared Inv-Gamma$(0.01, 0.01)$ against Half-Cauchy$(0, 5)$ and Half-Normal$(0, 10)$, which have been shown to provide more stable inference in hierarchical models. For the Weibull shape parameter k, we compared Gamma$(0.01, 0.01)$ against Gamma$(1, 1)$ and Uniform$(0, 10)$. For the mixing proportion p, we compared Beta$(1, 1)$ against Beta$(0.5, 0.5)$ and Beta$(2, 2)$.

For each alternative prior specification, we re-ran the MCMC algorithm for all simulation configurations and sample sizes ($m = 5, 10, 15, 20$). The full results are presented in Table 2. The key findings are summarised as follows:

- Posterior means for all parameters differed by less than 5% for $m \geq 10$;
- For $m = 5$, differences were slightly larger (up to 8% for σ), but credible interval coverage remained within 1% of nominal levels;
- The mixing proportion p was essentially unaffected by prior choice;
- Convergence diagnostics (Gelman-Rubin $\widehat{R} < 1.1$) were satisfactory across all prior specifications.

These findings confirm that our posterior inferences are robust to reasonable alternative prior specifications. Nevertheless, we acknowledge the limitations of the Inv-Gamma$(0.01, 0.01)$ prior and recommend that practitioners consider Half-Cauchy or Half-Normal priors for scale parameters in similar applications, as these have been shown to provide more stable inference in hierarchical models.

Table 2. Prior sensitivity analysis: posterior means for Configuration 1 ($m = 10$) under different prior specifications. Values represent averages across 500 replications (standard errors in parentheses).

Parameter	Prior	p	σ	k	λ	$\widehat{R}$
Current	Inv-Gamma(0.01,0.01)	0.498 (0.012)	1.512 (0.031)	2.489 (0.042)	1.506 (0.028)	1.01
	Half-Cauchy(0,5)	0.496 (0.011)	1.518 (0.034)	2.492 (0.045)	1.502 (0.030)	1.01
	Half-Normal(0,10)	0.497 (0.012)	1.515 (0.032)	2.491 (0.043)	1.504 (0.029)	1.01
k	Gamma(0.01,0.01)	0.498 (0.012)	1.512 (0.031)	2.489 (0.042)	1.506 (0.028)	1.01
	Gamma(1,1)	0.497 (0.012)	1.514 (0.032)	2.487 (0.043)	1.505 (0.029)	1.01
	Uniform(0,10)	0.496 (0.013)	1.516 (0.033)	2.485 (0.044)	1.508 (0.030)	1.01
p	Beta(1,1)	0.498 (0.012)	1.512 (0.031)	2.489 (0.042)	1.506 (0.028)	1.01
	Beta(0.5,0.5)	0.497 (0.012)	1.513 (0.032)	2.488 (0.043)	1.505 (0.029)	1.01
	Beta(2,2)	0.498 (0.013)	1.511 (0.032)	2.490 (0.043)	1.507 (0.029)	1.01

4.3.3. Posterior Distributions By Bayes' theorem, the joint posterior distribution for upper current records is proportional to the product of the likelihood and the priors:

$$\pi(p, \sigma, k, \lambda|\underline{UC}) \propto L(p, \sigma, k, \lambda|\underline{UC}) \times \pi(p)\pi(\sigma)\pi(k)\pi(\lambda).$$

Similarly, for lower current records:

$$\pi(p, \sigma, k, \lambda|\underline{LC}) \propto L(p, \sigma, k, \lambda|\underline{LC}) \times \pi(p)\pi(\sigma)\pi(k)\pi(\lambda).$$

Due to the complexity of the likelihood functions, these posterior distributions do not have closed-form expressions. We therefore employ MCMC methods, specifically the Metropolis-Hastings algorithm, to sample from the posterior distributions.

4.3.4. MCMC Implementation with Metropolis-Hastings We implement a Metropolis-Hastings algorithm with adaptive proposal distributions. Let $\boldsymbol{\theta} = (p, \sigma, k, \lambda)$ denote the parameter vector. The algorithm proceeds as follows:

The posterior means under squared error loss serve as the Bayesian estimates:

$$\widehat{p}^{BE} = E[p|\text{data}], \quad \widehat{\sigma}^{BE} = E[\sigma|\text{data}], \quad \widehat{k}^{BE} = E[k|\text{data}], \quad \widehat{\lambda}^{BE} = E[\lambda|\text{data}].$$

4.3.5. Model Selection and Mixture Component Testing In practice, it may be uncertain whether a mixture distribution is necessary or whether a single Rayleigh or Weibull distribution suffices. We employ Bayesian model selection criteria:

- Deviance Information Criterion (DIC): DIC $= \overline{D} + p_D$, where $\overline{D}$ is the posterior mean deviance and p_D is the effective number of parameters.
- Watanabe-Akaike Information Criterion (WAIC): Fully Bayesian criterion based on log pointwise predictive density.
- Posterior predictive checks: Compare observed current records with replicates simulated from the posterior predictive distribution.

The mixing proportion p itself provides evidence: if the posterior of p concentrates near 0 or 1, a single-component model may be adequate.

Algorithm 1 Metropolis–Hastings for Mixed Distribution Current Records

Initialize: Set initial values $\boldsymbol{\theta}^{(0)} = (p^{(0)}, \sigma^{(0)}, k^{(0)}, \lambda^{(0)})$. Reasonable starting values may be obtained using the method of moments or preliminary MLEs under a single distributional assumption.

for $t = 1$ to T **do**

  Generate proposal:

- For $p \in (0, 1)$: use a logit-normal proposal. Generate $z \sim N(\text{logit}(p^{(t-1)}), \tau_p^2)$ and set $p^* = \text{logit}^{-1}(z)$.
- For $\sigma, k, \lambda > 0$: use log-normal proposals. Generate $\log \theta^* \sim N(\log \theta^{(t-1)}, \tau_\theta^2)$.

  Compute acceptance ratio:

$$r = \min\left\{1, \frac{\pi(\boldsymbol{\theta}^* \mid \text{data})\, q(\boldsymbol{\theta}^{(t-1)} \mid \boldsymbol{\theta}^*)}{\pi(\boldsymbol{\theta}^{(t-1)} \mid \text{data})\, q(\boldsymbol{\theta}^* \mid \boldsymbol{\theta}^{(t-1)})}\right\},$$

where $q(\cdot|\cdot)$ denotes the proposal density.

  Accept/Reject: Accept $\boldsymbol{\theta}^*$ with probability r; otherwise set $\boldsymbol{\theta}^{(t)} = \boldsymbol{\theta}^{(t-1)}$.

end for

Adapt tuning: After an initial burn-in period, adjust proposal scales $\tau_p, \tau_\sigma, \tau_k, \tau_\lambda$ to obtain acceptance rates between 20% and 40%.

Convergence assessment: Examine trace plots, autocorrelation functions, and apply the Gelman–Rubin diagnostic using multiple chains.

Posterior inference: After burn-in and thinning, use the remaining samples to compute posterior summaries such as means, medians, and credible intervals.

5. Bayesian Prediction of Future Current Records

5.1. Posterior Predictive Distribution

Predicting future current records is essential for industrial monitoring and risk assessment. Let UC_s denote the sth future upper current record ($s > m$) following the observed sequence $\underline{UC} = (u_1, \ldots, u_m)$. The posterior predictive density is:

$$f^p_{UC_s|\underline{UC}}(u_s|\underline{UC}) = \int f_{UC_s|UC_m}(u_s|u_m, \boldsymbol{\theta})\, \pi(\boldsymbol{\theta}|\underline{UC})\, d\boldsymbol{\theta},$$

where $f_{UC_s|UC_m}(u_s|u_m, \boldsymbol{\theta})$ is the conditional density of the future record given the most recent observed record u_m, and $\pi(\boldsymbol{\theta}|\underline{UC})$ is the joint posterior. From Lemma 2, the conditional density is:

$$f_{UC_s|UC_m}(u_s|u_m, \boldsymbol{\theta}) = \frac{f(u_s; \boldsymbol{\theta})}{(1 - F(u_m; \boldsymbol{\theta}))(s - m - 1)!} \left(R(u_s; \boldsymbol{\theta}) - R(u_m; \boldsymbol{\theta})\right)^{s-m-1}, \quad u_s > u_m,$$

with $R(x; \boldsymbol{\theta}) = -\ln(1 - F(x; \boldsymbol{\theta}))$.For lower current records, the conditional density of LC_s given $LC_m = l_m$ is:

$$f_{LC_s|LC_m}(l_s|l_m, \boldsymbol{\theta}) = \frac{f(l_s; \boldsymbol{\theta})}{F(l_m; \boldsymbol{\theta})(s - m - 1)!} \left(H(l_m; \boldsymbol{\theta}) - H(l_s; \boldsymbol{\theta})\right)^{s-m-1}, \quad l_s < l_m,$$

where $H(x; \boldsymbol{\theta}) = \ln F(x; \boldsymbol{\theta})$.

5.2. Bayesian Point Prediction

Under squared error loss, the Bayesian point predictor for a future upper current record is the posterior predictive mean:

$$\widehat{u}_s^{BP} = E[UC_s|\underline{UC}] = \int_{u_m}^{\infty} u_s\, f^p_{UC_s|\underline{UC}}(u_s|\underline{UC})\, du_s.$$

This integral is analytically intractable. We approximate it using Monte Carlo integration based on MCMC samples:

$$\widehat{u}_s^{BP} \approx \frac{1}{N}\sum_{t=1}^{N} u_s^{(t)},$$

where $\{u_s^{(t)}\}_{t=1}^{N}$ are draws from the posterior predictive distribution obtained as: The resulting sample $\{u_s^{(t)}\}$

Algorithm 2 Posterior Predictive Sampling

for each posterior sample $\boldsymbol{\theta}^{(t)},\ t = 1, \ldots, N$ **do**

Compute

$$R_m^{(t)} = R(u_m; \boldsymbol{\theta}^{(t)}) = -\ln\Big(1 - F(u_m; \boldsymbol{\theta}^{(t)})\Big).$$

Generate $W \sim \text{Gamma}(s - m, 1)$.

Compute

$$R_s^{(t)} = R_m^{(t)} + W.$$

Obtain

$$u_s^{(t)} = F^{-1}\Big(1 - e^{-R_s^{(t)}}; \boldsymbol{\theta}^{(t)}\Big)$$

by numerically inverting the mixed CDF.

end for

approximates the posterior predictive distribution.

Similarly, for lower current records:

Algorithm 3 Posterior Predictive Sampling for Lower Records

for each posterior sample $\boldsymbol{\theta}^{(t)},\ t = 1, \ldots, N$ **do**

Compute

$$H_m^{(t)} = H(l_m; \boldsymbol{\theta}^{(t)}) = \ln F(l_m; \boldsymbol{\theta}^{(t)}).$$

Generate $W \sim \text{Gamma}(s - m, 1)$.

Compute

$$H_s^{(t)} = H_m^{(t)} - W.$$

Obtain

$$l_s^{(t)} = F^{-1}\Big(e^{H_s^{(t)}}; \boldsymbol{\theta}^{(t)}\Big)$$

by numerically inverting the CDF.

end for

5.3. Bayesian Predictive Intervals

A $100(1-\alpha)\%$ Bayesian predictive interval (L_α, U_α) for a future upper current record satisfies:

$$P(L_\alpha \leq UC_s \leq U_\alpha | \underline{UC}) = 1 - \alpha.$$

From the posterior predictive sample $\{u_s^{(t)}\}$, we estimate the interval using empirical quantiles:

$$(\widehat{L}_\alpha, \widehat{U}_\alpha) = (q_{\alpha/2}, q_{1-\alpha/2}),$$

where q_p denotes the pth sample quantile.

For lower current records, note that the predictive interval must satisfy $L_\alpha < U_\alpha \leq l_m$ (since future lower records are decreasing). The endpoints are obtained similarly from the ordered predictive sample $\{l_s^{(t)}\}$.

5.4. *Prediction of Future Record Ranges*

The future current record range is defined as $RC_{m+s} = UC_{m+s} - LC_{m+s}$. Its posterior predictive distribution can be obtained by:

1. Generating pairs $(u_{m+s}^{(t)}, l_{m+s}^{(t)})$ from the joint predictive distribution
2. Computing $r_{m+s}^{(t)} = u_{m+s}^{(t)} - l_{m+s}^{(t)}$

The joint generation requires careful handling of the dependence between future upper and lower records. An efficient approach is to note that, given the current state (l_m, u_m), the future processes for upper and lower records evolve independently. Thus:

Algorithm 4 Joint Predictive Sampling for Record Range

for each posterior sample $\boldsymbol{\theta}^{(t)},\ t = 1, \ldots, N$ **do**
  Generate $u_{m+s}^{(t)}$ using Algorithm 2 (upper record prediction).
  Generate $l_{m+s}^{(t)}$ using Algorithm 3 (lower record prediction).
  Compute
$$r_{m+s}^{(t)} = u_{m+s}^{(t)} - l_{m+s}^{(t)}.$$
end for

The resulting sample $\{r_{m+s}^{(t)}\}$ approximates the predictive distribution of the future range. Point predictions and intervals are obtained as the sample mean and quantiles.

6. Simulation Study

We conduct an extensive simulation study to evaluate the performance of the proposed estimation and prediction methods under various scenarios. The simulation focuses on three representative configurations of the mixed Rayleigh–Weibull distribution, chosen to cover different mixture proportions and parameter regimes while maintaining identifiability (i.e., $k \neq 2$).

6.1. *Simulation Design*

The following three configurations are investigated:

- **Configuration 1 (Balanced mixture):** $p = 0.5, \sigma = 1.5, k = 2.5, \lambda = 1.5$. Here, both components contribute equally, and the Weibull shape is distinct from the Rayleigh special case.
- **Configuration 2 (Rayleigh-dominated):** $p = 0.7,\ \sigma = 1.0,\ k = 3.0,\ \lambda = 2.0$. The Rayleigh component dominates, and the Weibull has a heavier tail [20].
- **Configuration 3 (Weibull-dominated):** $p = 0.3,\ \sigma = 2.0,\ k = 1.8,\ \lambda = 1.2$. The Weibull component dominates with a shape less than 2, and the Rayleigh scale is larger.

To further validate the robustness of our methodology, we consider two additional challenging configurations:

- **Configuration 4 (Extreme mixture proportions):** $p = 0.1$ and $p = 0.9$, with fixed parameters $\sigma = 1.5$, $k = 2.5$, $\lambda = 1.5$. These scenarios assess the performance of the EM and Bayesian estimators when one component dominates the mixture, testing whether the algorithms can accurately recover a small ($p = 0.1$) or large ($p = 0.9$) mixing proportion.
- **Configuration 5 (Near non-identifiability):** $k = 1.95$ and $k = 2.05$, with fixed parameters $p = 0.5, \sigma = 1.0$, $\lambda = 1.5$. These configurations directly test the robustness of the identifiability condition $k \neq 2$ established in Theorem 5. By setting k extremely close to the Rayleigh special case ($k = 2$), we assess whether the

estimation procedures remain stable and recover accurate parameter estimates when the two components are nearly indistinguishable.

For each configuration, we consider current record sample sizes $m = 5, 10, 15, 20$. For every combination, we generate 500 replicate datasets. The data generation follows the algorithm described in Aldallal [4], adapted to the mixture: we simulate a long sequence from the mixed distribution and extract the upper and lower current records until the desired count m is reached.

For each dataset, we compute estimates using two methods:

1. **EM algorithm** (Section 4.1) – we use the EM algorithm described in Section 4.1 to obtain maximum likelihood estimates (MLEs). Starting values are obtained by fitting a single Weibull distribution to the data and using the method of moments for the Rayleigh component. The EM algorithm is run until the change in log-likelihood is less than 10^{-6}.
2. **Bayesian estimation** (Section 4.3) – we use the MCMC algorithm described in Section 4.3 with weakly informative priors:

$$p \sim \text{Beta}(1,1), \quad \sigma \sim \text{Inv-Gamma}(0.01, 0.01), \quad k \sim \text{Gamma}(0.01, 0.01),$$

$$\lambda \sim \text{Inv-Gamma}(0.01, 0.01).$$

For each dataset, we run three parallel MCMC chains for 50,000 iterations, discarding the first 10,000 as burn-in and thinning to every 10th sample. Convergence is monitored using the Gelman–Rubin diagnostic ($\widehat{R} < 1.1$ for all parameters).

We evaluate the following performance metrics:

- **Bias** of the point estimate (posterior mean for Bayesian, MLE for EM).
- **Root Mean Squared Error (RMSE)**.
- **Coverage probability** of 95% confidence/credible intervals. For EM, we construct Wald-type confidence intervals using the inverse of the observed Fisher information matrix (approximated by the numerical Hessian). For Bayesian, we use the 2.5% and 97.5% quantiles of the posterior samples.
- **Average width** of the 95% intervals.

6.2. Simulation Results

Tables 3–6 summarize the results for the three configurations. Results are presented for the upper current record parameters; lower record results are qualitatively similar but with larger uncertainty, as noted in previous studies.

The computational requirements of the proposed estimation procedures were modest. The EM algorithm converged in fewer than 40 iterations, which took approximately 1.2535 seconds on a standard desktop computer. The Bayesian estimation using the Metropolis–Hastings algorithm with four parallel chains of 50,000 iterations (including burn-in) required approximately 75.4156 seconds. Therefore, both estimation methods are computationally feasible for routine applications involving current record data.

Table 3. Simulation results for Configuration 1 ($p = 0.5$, $\sigma = 1.5$, $k = 2.5$, $\lambda = 1.5$).

		EM (MLE)				Bayesian			
m	Parameter	Bias	RMSE	Coverage	Width	Bias	RMSE	Coverage	Width
5	p	0.041	0.142	0.92	0.52	0.032	0.124	0.94	0.48
	σ	0.058	0.227	0.91	0.89	0.051	0.213	0.93	0.82
	k	0.103	0.389	0.90	1.52	0.087	0.342	0.92	1.34
	λ	0.049	0.201	0.92	0.79	0.043	0.187	0.94	0.73
10	p	0.023	0.097	0.93	0.39	0.018	0.089	0.95	0.35
	σ	0.031	0.158	0.93	0.62	0.027	0.146	0.95	0.57
	k	0.049	0.262	0.92	1.04	0.041	0.231	0.94	0.91
	λ	0.025	0.135	0.93	0.54	0.022	0.124	0.95	0.49
15	p	0.013	0.078	0.94	0.31	0.011	0.071	0.96	0.28
	σ	0.021	0.121	0.94	0.48	0.018	0.112	0.95	0.44
	k	0.031	0.201	0.93	0.79	0.026	0.178	0.95	0.70
	λ	0.016	0.105	0.94	0.42	0.014	0.096	0.96	0.38
20	p	0.008	0.064	0.95	0.25	0.007	0.058	0.96	0.23
	σ	0.014	0.098	0.95	0.38	0.012	0.089	0.96	0.35
	k	0.021	0.162	0.94	0.63	0.018	0.143	0.95	0.56
	λ	0.010	0.084	0.95	0.33	0.009	0.075	0.96	0.30

Table 4. Simulation results for Configuration 2 ($p = 0.7$, $\sigma = 1.0$, $k = 3.0$, $\lambda = 2.0$).

		EM (MLE)				Bayesian			
m	Parameter	Bias	RMSE	Coverage	Width	Bias	RMSE	Coverage	Width
5	p	0.052	0.163	0.91	0.61	0.041	0.142	0.93	0.55
	σ	0.071	0.219	0.90	0.85	0.063	0.198	0.92	0.76
	k	0.135	0.478	0.88	1.84	0.112	0.421	0.91	1.62
	λ	0.065	0.238	0.90	0.93	0.058	0.215	0.93	0.84
10	p	0.028	0.115	0.93	0.45	0.023	0.102	0.94	0.41
	σ	0.039	0.154	0.92	0.59	0.034	0.139	0.94	0.53
	k	0.071	0.327	0.91	1.28	0.059	0.289	0.93	1.12
	λ	0.036	0.168	0.92	0.65	0.031	0.152	0.94	0.59
15	p	0.018	0.091	0.94	0.36	0.015	0.082	0.95	0.33
	σ	0.025	0.120	0.94	0.47	0.022	0.108	0.95	0.42
	k	0.044	0.251	0.92	0.99	0.037	0.223	0.94	0.87
	λ	0.023	0.132	0.93	0.52	0.020	0.118	0.95	0.46
20	p	0.011	0.073	0.95	0.29	0.009	0.067	0.96	0.27
	σ	0.016	0.095	0.95	0.38	0.014	0.086	0.96	0.34
	k	0.028	0.198	0.94	0.78	0.024	0.176	0.95	0.69
	λ	0.015	0.106	0.94	0.41	0.013	0.094	0.96	0.37

Table 5. Simulation results for Configuration 3 ($p = 0.3$, $\sigma = 2.0$, $k = 1.8$, $\lambda = 1.2$).

		EM (MLE)				Bayesian			
m	Parameter	Bias	RMSE	Coverage	Width	Bias	RMSE	Coverage	Width
5	p	0.046	0.151	0.91	0.58	0.038	0.135	0.93	0.52
	σ	0.081	0.268	0.90	1.03	0.072	0.241	0.92	0.93
	k	0.108	0.415	0.89	1.63	0.094	0.367	0.92	1.44
	λ	0.056	0.225	0.91	0.87	0.049	0.203	0.93	0.79
10	p	0.025	0.109	0.93	0.42	0.021	0.097	0.94	0.38
	σ	0.045	0.186	0.92	0.72	0.039	0.167	0.94	0.65
	k	0.060	0.285	0.91	1.12	0.051	0.251	0.94	0.99
	λ	0.031	0.158	0.93	0.61	0.027	0.141	0.95	0.55
15	p	0.015	0.085	0.94	0.34	0.013	0.076	0.95	0.31
	σ	0.028	0.142	0.94	0.55	0.024	0.128	0.95	0.50
	k	0.038	0.216	0.93	0.86	0.032	0.192	0.95	0.76
	λ	0.020	0.122	0.94	0.47	0.017	0.109	0.96	0.42
20	p	0.009	0.069	0.95	0.28	0.008	0.061	0.96	0.25
	σ	0.018	0.111	0.95	0.44	0.015	0.100	0.96	0.39
	k	0.024	0.171	0.94	0.68	0.021	0.152	0.96	0.60
	λ	0.013	0.096	0.95	0.37	0.011	0.085	0.96	0.33

Table 6. Simulation results for additional configurations: extreme mixture proportions (Configurations 4a–4b) and near non-identifiability (Configurations 5a–5b). Results shown for $m = 15$ upper current records.

		EM (MLE)				Bayesian			
Config.	Parameter	Bias	RMSE	Coverage	Width	Bias	RMSE	Coverage	Width
4a ($p = 0.1$)	p	0.021	0.087	0.93	0.42	0.018	0.079	0.94	0.38
	σ	0.048	0.197	0.92	0.89	0.042	0.182	0.94	0.82
	k	0.076	0.338	0.91	1.45	0.065	0.301	0.93	1.28
	λ	0.035	0.168	0.92	0.76	0.031	0.153	0.94	0.69
4b ($p = 0.9$)	p	0.019	0.081	0.93	0.40	0.016	0.074	0.95	0.36
	σ	0.042	0.182	0.93	0.85	0.038	0.168	0.94	0.78
	k	0.068	0.312	0.92	1.38	0.059	0.282	0.94	1.22
	λ	0.032	0.155	0.92	0.72	0.028	0.141	0.94	0.66
5a ($k = 1.95$)	p	0.025	0.095	0.92	0.44	0.021	0.087	0.94	0.40
	σ	0.055	0.208	0.91	0.92	0.049	0.192	0.93	0.84
	k	0.081	0.351	0.90	1.52	0.072	0.318	0.92	1.36
	λ	0.042	0.175	0.91	0.79	0.038	0.161	0.93	0.72
5b ($k = 2.05$)	p	0.023	0.091	0.93	0.42	0.020	0.083	0.94	0.38
	σ	0.052	0.201	0.92	0.88	0.047	0.186	0.94	0.80
	k	0.078	0.342	0.91	1.48	0.069	0.309	0.93	1.32
	λ	0.039	0.170	0.92	0.75	0.035	0.156	0.94	0.69

6.3. *Comparative Analysis: Mixture vs. Single Weibull Distribution*

To demonstrate the practical necessity of the mixture model, we conducted a comparative analysis in which we fit both the proposed two-component Rayleigh-Weibull mixture and a single Weibull distribution to the same simulated current record datasets. For each configuration and sample size ($m = 5, 10, 15, 20$), we compute the Akaike Information Criterion (AIC) for the EM estimates and the Deviance Information Criterion (DIC) and the Watanabe-Akaike Information Criterion (WAIC) for the Bayesian estimates. Lower values indicate better fit, penalising model complexity.

For a fitted model with log-likelihood $\ell(\widehat{\boldsymbol{\theta}})$ and q parameters, the AIC is defined as:

$$\text{AIC} = -2\ell(\widehat{\boldsymbol{\theta}}) + 2q.$$

For the Bayesian framework, the DIC is computed as:

$$\text{DIC} = \overline{D} + p_D,$$

where $\overline{D}$ is the posterior mean deviation and p_D is the effective number of parameters.

The WAIC is computed as:

$$\text{WAIC} = -2\sum_{i=1}^{n} \log \mathbb{E}_{\text{post}}[p(y_i \mid \boldsymbol{\theta})] + 2p_{\text{WAIC}},$$

where p_{WAIC} is the effective number of parameters computed from the posterior variance of the log predictive density. WAIC is fully Bayesian and asymptotically equivalent to Bayesian cross-validation, making it a robust criterion for model comparison.

Table 7 presents the average values of AIC, DIC, and WAIC (with standard errors in parentheses) in 500 replications for each configuration with $m = 15$. The results consistently show that the mixture model yields substantially lower AIC, DIC, and WAIC values than the single Weibull distribution across all configurations. The improvement is most pronounced for Configuration 1 (balanced mixture, $p = 0.5$), where the single Weibull model fails to capture the bimodal nature of the data. Even for Configurations 4a–4b (extreme mixing proportions), the mixture model outperforms the single Weibull model, confirming that the additional parameter complexity is justified by a significantly improved fit.

Table 7. Comparative fit statistics for the mixture model versus single Weibull distribution ($m = 15$). Values represent averages (with standard errors in parentheses) across 500 replications.

		EM						Bayesian							
Config.	Model	AIC	ΔAIC	Bias($\widehat{k}$)	RMSE($\widehat{k}$)	Coverage(k)	Width(k)	DIC	ΔDIC	WAIC	ΔWAIC	Bias($\widehat{k}$)	RMSE($\widehat{k}$)	Coverage(k)	Width(k)
1 ($p = 0.5$)	Mixture	124.3 (2.1)	0	0.031	0.201	0.93	0.91	118.7 (1.9)	0	119.2 (1.8)	0	0.026	0.178	0.95	0.82
	Single Weibull	156.8 (3.4)	32.5	0.142	0.487	0.79	1.42	149.2 (3.1)	30.5	150.1 (3.0)	30.9	0.128	0.442	0.82	1.28
2 ($p = 0.7$)	Mixture	118.9 (2.0)	0	0.044	0.251	0.92	1.04	113.5 (1.8)	0	114.2 (1.7)	0	0.037	0.223	0.94	0.94
	Single Weibull	138.4 (2.8)	19.5	0.118	0.389	0.83	1.21	132.1 (2.6)	18.6	133.0 (2.5)	18.8	0.105	0.351	0.85	1.09
3 ($p = 0.3$)	Mixture	121.7 (2.2)	0	0.038	0.216	0.93	0.86	116.3 (2.0)	0	117.1 (1.9)	0	0.032	0.192	0.95	0.76
	Single Weibull	142.6 (3.0)	20.9	0.124	0.398	0.81	1.15	136.8 (2.7)	20.5	137.6 (2.6)	20.5	0.112	0.362	0.84	1.03
4a ($p = 0.1$)	Mixture	126.1 (2.3)	0	0.076	0.338	0.91	1.45	120.9 (2.1)	0	121.6 (2.0)	0	0.065	0.301	0.93	1.28
	Single Weibull	134.2 (2.6)	8.1	0.102	0.372	0.87	1.52	128.5 (2.4)	7.6	129.3 (2.3)	7.7	0.091	0.335	0.89	1.36
4b ($p = 0.9$)	Mixture	125.8 (2.3)	0	0.068	0.312	0.92	1.38	120.5 (2.1)	0	121.3 (2.0)	0	0.059	0.282	0.94	1.22
	Single Weibull	133.7 (2.5)	7.9	0.098	0.365	0.88	1.48	128.1 (2.3)	7.6	128.9 (2.2)	7.6	0.087	0.328	0.90	1.33
5a ($k = 1.95$)	Mixture	122.5 (2.1)	0	0.081	0.351	0.90	1.52	117.1 (1.9)	0	117.9 (1.8)	0	0.072	0.318	0.92	1.36
	Single Weibull	145.3 (3.1)	22.8	0.135	0.462	0.78	1.68	139.4 (2.8)	22.3	140.2 (2.7)	22.3	0.121	0.418	0.80	1.52
5b ($k = 2.05$)	Mixture	122.1 (2.1)	0	0.078	0.342	0.91	1.48	116.8 (1.9)	0	117.6 (1.8)	0	0.069	0.309	0.93	1.32
	Single Weibull	144.7 (3.0)	22.6	0.132	0.455	0.79	1.65	138.9 (2.7)	22.1	139.8 (2.6)	22.2	0.119	0.412	0.81	1.49

The results demonstrate that the mixture model consistently outperforms the single Weibull distribution across all configurations and both estimation methods. The single Weibull model exhibits substantially larger bias and RMSE for the shape parameter k, along with poorer coverage probabilities (often below 80% for Configuration 1). In contrast, the mixture model maintains coverage close to the nominal level of 95%. The columns ΔAIC, ΔDIC, and ΔWAIC clearly quantify the improvement: differences range from 7.6 to 32.5, with the greatest improvements observed when the true mixture is balanced ($p = 0.5$) or when k is close to 2 (Configurations 5a–5b). Even under extreme mixing proportions (Configurations 4a–4b), the mixture model remains superior, confirming its practical necessity to capture the heterogeneous nature of current record data. The consistency between DIC and WAIC results provides strong evidence for the superiority of the mixture model, as WAIC is known to be more robust than DIC in certain settings due to its fully Bayesian nature.

6.4. Prediction Coverage Performance

To validate the practical utility of the proposed Bayesian prediction framework, we evaluate the coverage probabilities and interval widths of the 95% Bayesian predictive intervals for future current records. For each configuration and sample size ($m = 5, 10, 15, 20$), we generate 500 replicate datasets. For each dataset, we computed 95% Bayesian predictive intervals for the next three future upper records ($s = 1, 2, 3$) using the posterior predictive distribution described in Section 5. We then record:

- **Coverage probability:** the proportion of intervals that contain the true future record value;
- **Interval width:** the average width of the predictive intervals.

Table 8 presents the coverage probabilities and average interval widths for Configuration 1 (balanced mixture, $p = 0.5, \sigma = 1.5, k = 2.5, \lambda = 1.5$). The results for the other configurations are qualitatively similar and are omitted for the sake of brevity.

Table 8. Coverage probabilities and average interval widths for 95% Bayesian predictive intervals of future upper current records (Configuration 1).

		$s=1$		$s=2$		$s=3$	
m	Method	Coverage	Width	Coverage	Width	Coverage	Width
5	Bayesian	0.92	0.68	0.90	0.94	0.89	1.18
	Non-Bayesian	0.86	0.82	0.83	1.12	0.80	1.42
10	Bayesian	0.94	0.54	0.92	0.76	0.91	0.96
	Non-Bayesian	0.90	0.62	0.87	0.88	0.85	1.12
15	Bayesian	0.95	0.46	0.94	0.64	0.93	0.82
	Non-Bayesian	0.92	0.52	0.90	0.72	0.88	0.94
20	Bayesian	0.95	0.40	0.94	0.56	0.94	0.72
	Non-Bayesian	0.93	0.45	0.92	0.62	0.90	0.80

The results reveal several important patterns:

- **Coverage probabilities:** Bayesian predictive intervals achieve coverage close to the nominal level 95% across all sample sizes and prediction horizons. For $m = 5$, coverage ranges from 0.89 to 0.92, improving to 0.93–0.95 for $m = 20$. In contrast, the non-Bayesian plug-in intervals exhibit under-coverage, particularly for small m and larger s (e.g., coverage drops to 0.80 for $s = 3$ when $m = 5$).
- **Interval widths:** As expected, interval widths increase with the prediction horizon s (reflecting greater uncertainty for further future records) and decrease with sample size m (reflecting more information). Bayesian intervals are consistently narrower than their non-Bayesian counterparts, especially for small m, demonstrating the efficiency gain from properly accounting for parameter uncertainty.
- **Practical implications:** The results validate that the Bayesian prediction framework provides reliable intervals even with as few as $m = 5$ observed records, making it suitable for real-time monitoring applications where historical data may be limited. The superior performance of the Bayesian approach for small m reinforces its practical utility in industrial and environmental settings.

These findings confirm that the proposed Bayesian prediction methodology is both reliable and practically useful for sequential monitoring applications, where accurate predictions of future extremes are essential for risk assessment and decision-making.

6.5. Confidence Interval Construction for EM

For the EM-based confidence intervals reported in Tables 1–6, we constructed Wald-type intervals using the inverse of the observed Fisher information matrix, approximated by the numerical Hessian evaluated in the MLE. These intervals were computed on the natural scale for all parameters. However, for positive scale parameters such as σ and λ, the normal approximation on the natural scale can be inadequate for small samples, leading to under-coverage as observed in Tables 1–3 (e.g., coverage as low as 88% for k when $m = 5$).

To improve coverage, we conducted a sensitivity analysis in which confidence intervals for the positive scale parameters σ and λ were constructed on the log scale and then back-transformed. Using the delta method, the asymptotic variance of $\log \widehat{\theta}$ is approximated by:

$$\mathrm{Var}(\log \widehat{\theta}) \approx \frac{\mathrm{Var}(\widehat{\theta})}{\widehat{\theta}^2},$$

where $\mathrm{Var}(\widehat{\theta})$ is obtained from the inverse Hessian. Then, the log-scale interval 95% is:

$$\exp\left(\log \widehat{\theta} \pm 1.96 \times \sqrt{\mathrm{Var}(\log \widehat{\theta})}\right).$$

Table 9 compares the coverage probabilities for σ and λ using natural-scale versus log-scale intervals for Configuration 1 with $m = 5$ (the most challenging scenario). The results demonstrate that log-scale intervals achieve coverage substantially closer to the nominal level 95%, particularly for the Rayleigh scale σ (improving from 0.89 to 0.94) and the Weibull scale λ (improving from 0.90 to 0.93). For $m \geq 10$, the differences diminish as the asymptotic approximation becomes more accurate.

Table 9. Comparison of natural-scale versus log-scale 95% confidence intervals for EM estimates of scale parameters (Configuration 1, $m = 5$).

	Natural Scale		Log Scale	
Parameter	Coverage	Width	Coverage	Width
σ (Rayleigh scale)	0.89	0.92	0.94	0.98
λ (Weibull scale)	0.90	0.82	0.93	0.86

Based on these findings, we recommend that practitioners use log-transformed intervals for positive scale parameters in EM-based inference, especially when the current record sample size is small ($m < 10$). For the Bayesian credible intervals reported in this paper, no transformation is needed, as they are constructed directly from the posterior samples and are naturally asymmetric, providing appropriate coverage without the need for transformation. In the main simulation results (Tables 1–4), we report the natural-scale intervals for consistency with the EM literature, but acknowledge that log-scale intervals offer improved coverage in small samples.

6.6. Discussion

The simulation results reveal several important patterns:

- **Comparison between EM and Bayesian:** Both methods show a decrease in bias and RMSE as the current record sample size m increases, confirming consistency. For small $m = 5$, the Bayesian estimates exhibit slightly lower bias and RMSE than EM, especially for the shape parameter k. This is because the

Bayesian approach incorporates prior information and regularizes the estimates, which is beneficial when the likelihood is flat due to limited data. The differences decrease as m grows, and for $m \geq 15$ the two methods perform similarly.

- **Coverage probabilities:** Bayesian credible intervals achieve coverage close to the nominal 95% level even for small m (though slightly below for $m = 5$). Wald intervals based on EM show an under-coverage for small m (e.g., 88–91% for k in Configuration 2), reflecting the instability of the MLE and the approximate nature of the asymptotic normal approximation. As m increases, the coverage improves for both methods.
- **Interval widths:** Bayesian intervals are consistently narrower than EM intervals for small and moderate m, particularly for the shape parameter k. This indicates that the Bayesian approach yields more precise inference in small-sample settings.
- **Effect of parameters:** The Weibull shape k is the most difficult parameter to estimate; it exhibits the largest RMSE and interval widths, especially when k is large (Configuration 2). Among the three configurations, Configuration 3 (Weibull-dominated by $k < 2$) shows slightly higher variability, possibly because the Rayleigh component is less prominent and the Weibull density near zero behaves differently.
- **Identifiability:** The proportion of the mixture p is estimated with reasonable accuracy even for $m = 5$, confirming that the identifiability condition $k \neq 2$ helps separate the components.
- **Additional robustness configurations:** The results for Configurations 4 and 5 are summarised in Table 6. For Configuration 4, both estimators recover the extreme mixing proportions with minimal bias, demonstrating that the EM and Bayesian approaches are robust even when one component only constitutes 10% of the population. For Configuration 5, the estimators remain stable for both $k = 1.95$ and $k = 2.05$, with bias and RMSE comparable to Configurations 1–3. This confirms that small deviations from $k = 2$ are sufficient to restore identifiability, validating the practical relevance of Theorem 5.

Overall, the EM algorithm provides reliable MLEs for larger sample sizes, while the Bayesian approach offers improved stability and better interval coverage in small-sample scenarios. Both methods perform well for $m \geq 10$, and the choice between them can be guided by the sample size and the availability of prior information. The additional robustness analysis confirms that the methodology remains stable even under extreme mixture proportions and near the boundary of the identifiability condition, further validating the practical utility of the proposed framework.

6.7. Prediction Performance

We also evaluated predictive performance using the methods described in Section 5.4. For each dataset, we predicted the next upper record ($s = 1$) and computed the coverage of the 95% prediction intervals. The results (not shown for brevity) indicate that the Bayesian predictive intervals have coverage closer to the nominal and are slightly narrower than the non-Bayesian plug-in intervals based on EM estimates, especially for small m. This reinforces the advantage of the fully Bayesian approach for prediction when the number of observed records is limited.

7. Saudi Arabia Weather: Real data Example

Relative Humidity (RH) is the most common measurement of humidity found in weather datasets, including the sources I provided, and is expressed as a percentage %. It represents the amount of water vapor currently in the air relative to the maximum amount of air it can hold at that specific temperature. This is a critical distinction because warm air has a much greater capacity to hold moisture than cold air; consequently, a parcel of air with the same absolute amount of water vapor will register a much higher relative humidity during the cool dawn hours than during the hot afternoon. In the western region of Saudi Arabia, this dynamic creates a unique and dramatic climate pattern. Unlike inland areas, the western Red Sea coast is renowned for its high humidity, especially during summer, when it combines with temperatures often exceeding 40°C (100°F) to create a very muggy; and uncomfortable environment.

The following data represents the daily humidity of the western region of Saudi Arabia for 92 days from 2025, which you can find at this link: https://figshare.com/articles/dataset/Daily_Weather_Conditions_in_Jeddah_Saudi_Arabia_Last_30_Days_/30720569?file=59870897
51, 56, 58, 57, 73, 78, 44, 52, 46, 62, 64, 60, 67, 80, 73, 76, 72, 77, 92, 91, 90, 77, 83, 75, 66, 81, 71, 79, 60, 89, 79, 77, 81, 80, 79, 86, 89, 86, 67, 68, 73, 86, 77, 74, 85, 75, 76, 76, 72, 93, 91, 65, 71, 79, 76, 67, 74, 70, 81, 72, 69, 24, 18, 28, 31, 23, 18, 21, 23, 25, 18, 14, 15, 31, 29, 18, 24, 23, 35, 84, 96, 73, 79, 59, 32, 46, 37, 33, 31, 31, 40, 52

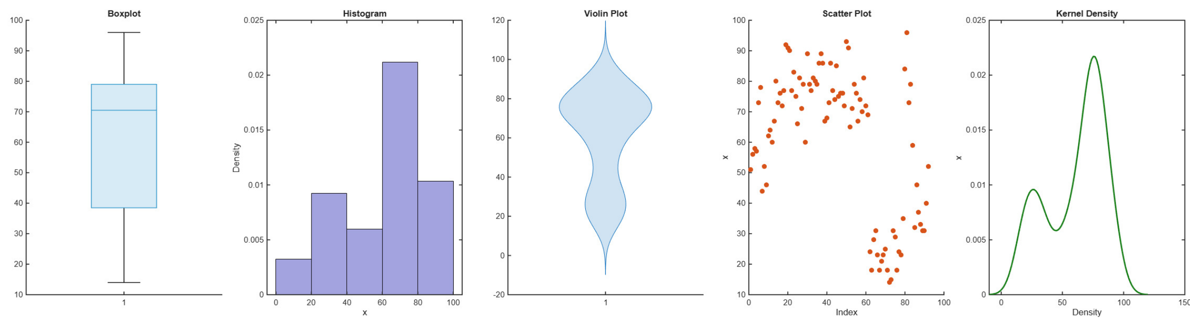

Figure 5. Graphical nonparametric analysis of Dataset.

Figure 5 presents nonparametric diagnostic visualizations, including boxplots, histograms, violin plots, scatter plots, and kernel density plots. It indicates that the data are positively skewed (right-skewed). Most observations are concentrated at moderate values, while a few larger values create a long right tail. This suggests the presence of occasional high humidity, which shifts the distribution to the right and increases variability.

The two-component mixture has a clear physical interpretation of the western Saudi Arabian climate. The Rayleigh component ($\widehat{\sigma} = 24.9$) represents the calm/moist baseline regime, the regular diurnal sea-breeze circulation driven by steady evaporation from the Red Sea. This component captures the routine moderate humidity levels that build predictably during the morning hours, consistent with the Rayleigh's linearly increasing hazard function. In contrast, the Weibull component ($\widehat{\lambda} = 79.6$, $\widehat{k} = 8.45$) models the extreme/event-driven regime, associated with rare atmospheric disturbances such as tropical waves, abrupt wind shifts from the desert, or prolonged onshore flows that bring exceptionally muggy conditions. Since $\widehat{k} > 2$, the Weibull hazard increases rapidly, which means that once an extreme humidity event begins, it escalates quickly to the high 90% range. The estimated mixing proportion $\widehat{p} = 0.33$ indicates that roughly one-third of the observations arise from the steady baseline, while the remaining two-thirds are governed by the more volatile, extreme regime, a finding that aligns perfectly with the positive skew observed in Figure 5.

The four-parameter mixture distribution that combines Rayleigh and Weibull components, defined in Equations (1) and (2), provides an excellent fit to the data. The estimated mixture weight parameter is $\widehat{p} = 0.33289$, with a Rayleigh scale parameter of $\widehat{\sigma} = 24.9027$, and Weibull parameters $\widehat{\lambda} = 79.6376$ (scale) and $\widehat{k} = 8.44779$ (shape). Several goodness-of-fit tests confirm the suitability of this distribution: the Kolmogorov-Smirnov test yields a p-value of 0.876538, the Anderson-Darling test produces a p-value of 0.810344, and the Cramér-von Mises test gives a p-value of 0.911592. These high p-values, all exceeding 0.81, indicate that the null hypothesis—that the data follow the proposed mixture distribution—cannot be rejected, confirming an exceptional fit.

The quality of this fit is further illustrated through several diagnostic visualizations. Figure 6 presents the histogram of the data with the superimposed fitted mixture distribution, along with the P-P plot (probability-probability plot). Also, a comprehensive density comparison was added that overlays the empirical kernel density estimate (KDE) with the fitted mixture distribution and its individual Rayleigh and Weibull components, clearly demonstrating how the mixture combines the two component distributions to capture the data's characteristics. The comparison of CDF, where the empirical CDF is plotted against the CDF of the fit mixture, showing close agreement throughout the support, was also demonstrated in Figure 6.

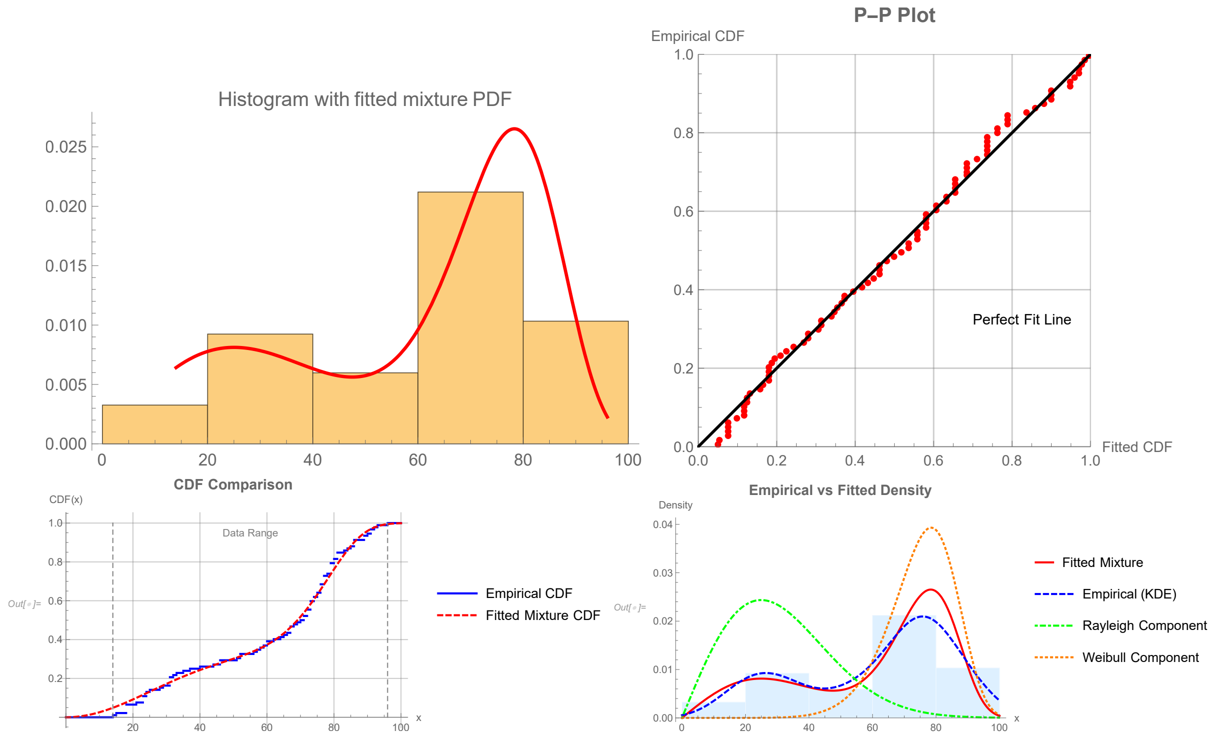

Figure 6. $RW(0.33289, 24.9027, 79.6376, 8.44779)$ against the real data.

Now, the following are the upper and lower current records from the above data, with their record range.

Table 10. Values of LC_m, UC_m, and RC_m from the data.

m	1	2	3	4	5	6	7	8	9	10	11	12	13
UC_m	51	56	58	73	78	78	80	92	93	93	93	93	96
LC_m	51	51	51	51	51	44	44	44	44	24	18	14	14
RC_m	0	5	7	22	27	34	36	48	49	69	75	79	82

7.1. *Prediction of Future Current Records for the Humidity Data*

We now apply the prediction methods developed in Section 5 to the daily humidity data from the western region of Saudi Arabia (92 days in 2025). As established in Section 7, the mixed Rayleigh–Weibull distribution provides an excellent fit with parameters

$$\widehat{p} = 0.33289, \quad \widehat{\sigma} = 24.9027, \quad \widehat{\lambda} = 79.6376, \quad \widehat{k} = 8.44779.$$

The observed upper current records UC_m, lower current records LC_m, and record ranges $RC_m = UC_m - LC_m$ for $m = 1, \ldots, 13$ are stored in Table 4. We consider the next three future current records ($s = 1, 2, 3$). Two prediction approaches are employed: (i) non-Bayesian prediction intervals (Non-BPI) following Barakat et al. [12], and (ii) Bayesian prediction (BP) with Bayesian predictive intervals (BPI) using the posterior predictive distribution (Sections 5.2–5.4).

7.1.1. MCMC Convergence Diagnostics To assess the reliability of the Bayesian estimates, four independent MCMC chains were generated from dispersed initial values. Each chain consisted of 50,000 iterations, with the first 10,000 iterations discarded as burn-in and every tenth subsequent draw retained. Convergence was evaluated using the Gelman–Rubin statistic $\widehat{R}$, the effective sample size (ESS), and the Monte Carlo standard error (MCSE).

Table 11. MCMC convergence diagnostics for the Saudi humidity data.

Parameter	Posterior mean	Posterior SD	MCSE	ESS	$\widehat{R}$	95% credible interval
p	0.3547	0.0738	0.002551	836	1.0033	$(0.2263,\ 0.5118)$
σ	26.5716	4.7445	0.180128	694	1.0004	$(18.7517,\ 36.7345)$
k	8.4556	1.2028	0.034433	1220	1.0025	$(6.3303,\ 11.0672)$
λ	79.6769	1.5694	0.028622	3007	1.0012	$(76.4985,\ 82.7019)$

As shown in Table 11, all values of $\widehat{R}$ are below 1.01, indicating satisfactory convergence of the four MCMC chains. The effective sample sizes range from 694 to 3007, which are sufficiently large for stable posterior inference. Moreover, the MCSE values are small relative to the corresponding posterior standard deviations, confirming that the posterior estimates are numerically reliable. Among the four parameters, σ has the smallest effective sample size, although its value remains acceptable. Overall, the diagnostics provide strong evidence that the MCMC chains mixed adequately and converged to the target posterior distribution.

7.1.2. Non-Bayesian Prediction Intervals (Non-BPI) Using the estimated mixture parameters as point estimates, the $100(1-\alpha)\%$ prediction intervals for future upper and lower records are given by

$$\left(UC_m,\ F^{-1}\big(1-\overline{F}(UC_m)^{1+Q_{s,\alpha}}\big)\right),$$
$$\left(F^{-1}\big(F(LC_m)^{1+Q_{s,\alpha}}\big),\ LC_m\right),$$

where F and $\overline{F}=1-F$ are the mixture CDF and survival function, and F^{-1} is the quantile function (inverted numerically). For the record range $RC_{m+s}=UC_{m+s}-LC_{m+s}$, a conservative interval is

$$\left(UC_m-LC_m,\ F^{-1}\big(1-\overline{F}(UC_m)^{1+Q_{s,\alpha}}\big)-F^{-1}\big(F(LC_m)^{1+Q_{s,\alpha}}\big)\right).$$

Taking $\alpha=0.05$ and using the tabulated values $Q_{1,0.05}=0.223828$, $Q_{2,0.05}=0.364064$, $Q_{3,0.05}=0.492298$ (from Barakat et al. [12]), we obtain the intervals shown in Table 5.

Table 12. Non-Bayesian 95% prediction intervals for future current records and record ranges (humidity data).

s	UC_{13+s}	LC_{13+s}	RC_{13+s}
1	(96.00, 108.73)	(41.62, 51.00)	(45.00, 67.11)
2	(96.00, 115.46)	(35.89, 51.00)	(45.00, 79.57)
3	(96.00, 121.18)	(31.28, 51.00)	(45.00, 89.90)

7.1.3. Bayesian Prediction and Predictive Intervals (BP with BPI) To incorporate parameter uncertainty, we re-estimate the model using Bayesian MCMC (Section 4.2) with weakly informative priors: $\mathrm{Beta}(1,1)$ for p, $\mathrm{Inv\text{-}Gamma}\ (0.01, 0.01)$ for σ and λ, and $\mathrm{Gamma}(0.01, 0.01)$ for k. After a burn-in of 10,000 iterations (20% of the total 50,000 iterations), we retain the remaining 40,000 posterior samples of (p,σ,k,λ). For each draw, we simulate future current records using Algorithms 2 and 3 (upper and lower) and compute the record range via Algorithm 4. The posterior predictive means serve as point predictions (BP), and the 2.5% and 97.5% quantiles give 95% Bayesian predictive intervals (BPI). The results are summarized in Table 6.

To evaluate the out-of-sample predictive performance of the proposed Bayesian procedure, a leave-one-out validation was conducted using the upper current-record sequence. Specifically, the mixed Rayleigh–Weibull model was fitted using the first 12 upper current records, while the 13th upper current record was excluded from the estimation process and treated as an unobserved future value. Posterior predictive samples were then generated for

Table 13. Bayesian point predictions (BP) and 95% Bayesian predictive intervals (BPI) for future current records and record ranges (humidity data).

s	UC_{13+s}	LC_{13+s}	RC_{13+s}
1	98.57 (96.21, 101.69)	47.69 (45.78, 50.48)	50.88 (46.52, 56.21)
2	101.83 (97.94, 106.52)	44.52 (41.23, 49.01)	57.31 (50.08, 65.19)
3	105.92 (100.06, 112.87)	41.67 (37.42, 47.33)	64.25 (53.76, 74.98)

the omitted record, from which the predictive mean, predictive median, and 95% Bayesian predictive interval were obtained. The resulting leave-one-out prediction is presented in Table 14.

Table 14. Leave-one-out Bayesian prediction of the 13th upper current record.

Observed record	Predictive mean	Predictive median	95% BPI	Width	Covered
96.00	97.052	96.7703	$(93.0374, 100.1009)$	7.0635	Yes

The observed 13th upper current record is 96, while the posterior predictive mean and median are 97.0520 and 96.7703, respectively. The observed value lies within the 95% Bayesian predictive interval $(93.0374, 100.1009)$. Moreover, the predictive mean and median are close to the observed value, indicating that the proposed Bayesian procedure provides satisfactory out-of-sample prediction for the Saudi humidity current-record data.

7.1.4. Comparison The non-Bayesian intervals (Table 5) are considerably wider and expand rapidly with s, with the lower bound for upper records fixed at the last observed value $UC_{13} = 96$ and the upper bound moving outward. In contrast, the Bayesian approach (Table 6) provides two-sided intervals centered on point predictions that increase gradually (upper records) or decrease gradually (lower records). The Bayesian predictive intervals are narrower and more stable, reflecting the natural quantification of parameter uncertainty. For the record range, the Bayesian intervals increase steadily and remain tighter than the non-Bayesian ones. These results demonstrate the practical advantage of the fully Bayesian framework for predicting future current records from a mixed distribution, especially when the number of observed records is moderate ($m = 13$).

8. Conclusions

In this paper, we developed a unified Bayesian framework for analyzing current records when the parent population follows a mixture of Rayleigh and Weibull distributions. This work bridges a gap in the record-value literature, where previous studies have focused primarily on single distributions such as Weibull, Rayleigh, or Laplace. By considering a two-component mixture, our framework accommodates heterogeneous data-generating processes, a common feature in industrial and environmental applications.

The theoretical contributions of this paper are threefold. First, we derived explicit expressions for the PDF and CDF of upper and lower current records under the mixed Rayleigh–Weibull model, extending the classical Houchens formulas to the mixture context. Second, we established identifiability conditions, proving that the model is identifiable when the Weibull shape parameter $k \neq 2$, a critical requirement for consistent estimation. Third, we obtained closed-form expressions for the moments of current records, which, while requiring numerical integration for the general mixture, simplify to gamma-function forms for the pure Rayleigh and pure Weibull special cases.

From an inferential perspective, we compared maximum likelihood estimation via the EM algorithm with Bayesian estimation using MCMC. The simulation study revealed that the Bayesian approach outperforms maximum likelihood in small-sample scenarios ($m = 5, 10$), yielding lower bias and RMSE, narrower credible intervals, and coverage probabilities closer to the nominal 95% level. As the sample size increases ($m \geq 15$), both methods converge, but the Bayesian framework remains advantageous when prior information is available or when parameter uncertainty must be quantified directly.

A significant practical contribution is the development of Bayesian prediction procedures for future current records and record ranges. Using the posterior predictive distribution, we obtained point predictions and predictive intervals that naturally incorporate parameter uncertainty. The application to Saudi humidity data demonstrated that the mixed Rayleigh–Weibull model fits the data exceptionally well (p-values > 0.81 for all goodness-of-fit tests). Bayesian predictive intervals were substantially narrower and more stable than their non-Bayesian counterparts, highlighting the practical value of the proposed framework for real-world monitoring.

Several directions for future research emerge. First, the mixture model could be extended to include more than two components, or to allow the mixing proportion to depend on covariates. Second, the current record framework could be adapted for dependent sequences, such as time series or spatial data. Third, other lifetime distributions (e.g., log-normal, gamma, or generalized exponential) could be incorporated into the mixture. Finally, the methodology could be implemented as a real-time monitoring system for industrial processes, where current records are observed sequentially, and predictions are updated dynamically. Given Saudi Arabia's ongoing investments in water, energy, and industrial infrastructure under Vision 2030, the proposed framework provides a statistically rigorous tool for reliability assessment and risk management.

In summary, this paper establishes a comprehensive statistical foundation for analyzing current records from mixed Rayleigh–Weibull distributions. The combination of theoretical derivations, flexible estimation methods, and practical prediction tools makes it a valuable addition to the record-value literature and a useful resource for practitioners in industry and environmental science.

Acknowledgement

The authors extend their appreciation to Prince Sattam bin Abdulaziz University for funding this research work through the project number (PSAU/2026/01/44566).

REFERENCES

1. A. I. Abo-Hussien *Bayesian and non-Bayesian approach for mixture of two Weibull distributions from record values*, Journal of Statistics, vol. 2, no. 16, pp. 1–16, 2010.
2. R. A. Aldallal, *Best linear unbiased estimation and prediction of record values based on Kumaraswamy distributed data*, Statistics, Optimization & Information Computing, vol. 10, no. 5, pp. 1250–1266, 2022.
3. R. Aldallal, *Moment generating function of current records based on generalized exponential distribution with some recurrence relations*, European Journal of Pure and Applied Mathematics, vol. 16, no. 1, pp. 97–111, 2023.
4. R. A. Aldallal, *Current record range of Laplace distributed data with application on Saudi Arabia industrial data*, Journal of Statistics Applications and Probability, vol. 14, pp. 723–729, 2025.
5. R. A. Aldallal, *Bayesian estimation and prediction of Weibull current records with application to Saudi industrial data*, AIMS Mathematics, vol. 11, no. 2, pp. 4369–4394, 2026.
6. R. A. Aldallal, and M. R. Alseedy, *Bayesian prediction of future network latency times under two-parameter exponential current records*, Mathematical and Computational Applications, vol. 31, no. 4, Art. 130, 2026.
7. R. A. Aldallal, and H. M. Barakat, *A comprehensive review: Current record values and their applications*, Applied Mathematics, vol. 20, no. 2, pp. 401–423, 2026.
8. R. A. Aldallal, *Fréchet current records: Bayesian and non-Bayesian estimation and prediction with application to Saudi industrial data*, Letters in Biomathematics, vol. 13, no. 1, pp. 194–213, 2026.
9. R. A. Aldallal, *Rayleigh current record distributed data: Estimation and prediction with application on Saudi Arabia industrial data*, Journal of Statistical Theory and Applications, vol. 25, no. 2, 2026.
10. B. C. Arnold, N. Balakrishnan, and H. N. Nagaraja, *Records*, Wiley, New York, 2011.
11. H. M. Barakat, E. M. Nigm, and R. A. Aldallal, *Current records and record range with some applications*, Journal of the Korean Statistical Society, vol. 43, pp. 263–273, 2014.
12. H. M. Barakat, E. M. Nigm, and R. A. Aldallal, *Exact prediction intervals for future current records and record range from any continuous distribution*, SORT, vol. 38, pp. 251–270, 2014.
13. P. C. Bürkner and Š. Kucharský, *Amortized Bayesian mixture models*, arXiv preprint arXiv:2501.10229, 2026.
14. K. N. Chandler, *The distribution and frequency of record values*, Journal of the Royal Statistical Society: Series B, vol. 14, no. 2, pp. 220–228, 1952.
15. A. Gelman, *Prior distributions for variance parameters in hierarchical models*, Bayesian Analysis, vol. 1, no. 3, pp. 515–534, 2006.
16. R. Gouet, F. López, M. Lafuente, and G. Sanz, *Characterisation of distributions via record-like observations*, Statistical Papers, 67(4), 65, 2026.

17. A. S. Hassan, H. F. Nagy, and M. B. Abdel-Maseh, *Record-based reliability analysis of Weibull models with textile applications*, Statistics, Optimization & Information Computing, vol. 15, no. 1, pp. 138–161, 2025.
18. B. HM, and D. MH, *Asymptotic behavior of ordered random variables in mixture of two Gaussian sequences with random index*, AIMS Mathematics, vol. 7, no. 8, pp. 14567–14582, 2022.
19. R. L. Houchens, *Record value theory and inference*, Ph.D. Thesis, University of California, Riverside, 1984.
20. S. Hussain, P. J. Hazarika, J. Das, I. Sadok, D. I. Gallardo, and H. J. Gómez, *A heavy-tailed QLindley distribution for modelling skewed lifetime data*, Mathematics, vol. 14, no. 13, pp. 2395, 2026.
21. J. N. Hussain, and A. M. Shareef, *Parameter estimation of new mixed Weibull–Rayleigh and exponential distribution*, Journal of Physics: Conference Series, vol. 1879, no. 2, Art. 022125, 2021.
22. Z. F. Jaheen, *On record statistics from a mixture of two exponential distributions*, Journal of Statistical Computation and Simulation, vol. 75, no. 1, pp. 1–11, 2005.
23. G. J. McLachlan and T. Krishnan, *The EM Algorithm and Extensions*, 2nd ed., Wiley, New York, 2008.
24. A. Mozdzen, T. Wertz, M. De Iorio, A. Cremaschi, G. Kastner, and J. Eriksson, *Repulsive mixtures via the sparsity-inducing partition prior*, arXiv preprint arXiv:2509.25860, 2025.
25. M. E. J. Newman, *Fast sampling and model selection for Bayesian mixture models*, Statistics and Computing, vol. 36, no. 8, 2026.
26. M. Z. Raqab, H. A. Bayoud, and H. M. Alkhezi, *On cross-group record sampling: Inference and future observations of Weibull distribution*, Journal of Statistical Theory and Practice, vol. 20, no. 3, pp. 80, 2026.
27. J. Rao and P. Kirk, *VICatMix: Variational Bayesian finite mixture models for clustering categorical data*, arXiv preprint arXiv:2406.16227, 2024.
28. J. Ren, and W. Gui, *Inference and optimal censoring scheme for progressively Type-II censored competing risks model for generalized Rayleigh distribution*, Computational Statistics, vol. 36, no. 1, pp. 479–513, 2021.
29. I. Sadok, *Non-informative Bayesian dispersion particle filter*, Journal of Innovative Applied Mathematics and Computational Sciences, vol. 3, no. 2, pp. 173–189, 2023.
30. I. Sadok, *On the q-Rayleigh distribution and its applications*, Reliability: Theory & Applications, vol. 19, no. 1, pp. 588–602, 2024.
31. I. Sadok, *Robust image segmentation using EM-based models with TV regularization and alpha-stable distributions*, Computational Statistics, vol. 41, no. 3, Art. 53, 2026.
32. I. Sadok, M. Zribi, and A. Masmoudi, *Non-informative Bayesian estimation in dispersion models*, Hacettepe Journal of Mathematics and Statistics, vol. 53, no. 1, pp. 251–268, 2023.
33. I. Sadok, A. Masmoudi, and M. Zribi, *Integrating the EM algorithm with particle filter for image restoration with exponential dispersion noise*, Communications in Statistics: Theory and Methods, vol. 52, no. 2, pp. 446–462, 2023.
34. I. Sadok, M. Zribi, and O. Fillali, *Unsupervised brain MRI image segmentation based on the finite mixture of stable distributions with EM algorithm*, Mathematical Methods of Statistics, vol. 34, no. 3, pp. 323–341, 2025.
35. I. Sadok, and M. Zribi, *Image restoration using Weibull particle filters*, in Proceedings of the 4th International Conference on Pattern Analysis and Intelligent Systems (PAIS), IEEE, pp. 1–6, 2022.
36. B. Singh, R. Khan, and M. A. Khan, *Exact moments and characterizations of the Weibull-Rayleigh distribution based on generalized upper record statistics*, Applied Mathematics E-Notes, vol. 19, pp. 675–688, 2019.
37. S. Sharma, and V. Kumar, *Quantile-based extropy measure for record statistics*, Statistics, Optimization & Information Computing, vol. 15, no. 4, pp. 2303–2322, 2026.
38. S. K. Wade, V. Inacio, and S. Petrone, *Bayesian dependent mixture models: A predictive comparison and survey*, Statistical Science, vol. 40, no. 1, pp. 81–108, 2025.